

MODELING PRIMORDIAL GAS IN  
NUMERICAL COSMOLOGY

Tom Abel, Peter Anninos, Yu Zhang & Michael L. Norman

Laboratory for Computational Astrophysics at the National Center for Supercomputing Applications

abel@astro.uiuc.edu

panninos@ncsa.uiuc.edu

yzhang@ncsa.uiuc.edu

norman@ncsa.uiuc.edu

Received \_\_\_\_\_; accepted \_\_\_\_\_

arXiv:astro-ph/9608040v1 9 Aug 1996

## ABSTRACT

We have reviewed the chemistry and cooling behaviour of low-density ( $n < 10^4 \text{ cm}^{-3}$ ) primordial gas and devised a cooling model which involves 19 collisional and 9 radiative processes and is applicable for temperatures in the range ( $1\text{K} < T < 10^8\text{K}$ ). We derived new fits of rate coefficients for the photo-attachment of neutral hydrogen, the formation of molecular hydrogen via  $\text{H}^-$ , charge exchange between  $\text{H}_2$  and  $\text{H}^+$ , electron detachment of  $\text{H}^-$  by neutral hydrogen, dissociative recombination of  $\text{H}_2^+$  with slow electrons, photodissociation of  $\text{H}_2^+$ , and photodissociation of  $\text{H}_2$ . Further it was found that the molecular hydrogen produced through the gas-phase processes,  $\text{H}_2^+ + \text{H} \rightarrow \text{H}_2 + \text{H}^+$ , and  $\text{H}^- + \text{H} \rightarrow \text{H}_2 + \text{e}^-$ , is likely to be converted into its para configuration on a faster time scale than the formation time scale. We have tested the model extensively and shown it to agree well with former studies. We further studied the chemical kinetics in great detail and devised a minimal model which is substantially simpler than the full reaction network but predicts correct abundances. This minimal model shows convincingly that 12 collisional processes are sufficient to model the H, He,  $\text{H}^+$ ,  $\text{H}^-$ ,  $\text{He}^+$ ,  $\text{He}^{++}$ , and  $\text{H}_2$  abundances in low density primordial gas for applications with no radiation fields.

## 1. Introduction

Since Szalay (1967) realized the importance of the gas phase reactions for  $\text{H}_2$  formation in primordial gas



and



and Peebles and Dicke (1968) formulated their theory for globular cluster formation based on  $\text{H}_2$  cooling of collapsing primordial density fluctuations, many models have been put forward employing this effect to explain the origin of structures on a vast range of mass scales. E.g., for the cosmic string model of structure formation, molecular hydrogen is believed to trigger the fragmentation of late cosmic string wakes. This is because, for the weak accretion shocks encountered during the formation of late cosmic string wakes, thermal instabilities due to hydrogen line, or bremsstrahlung cooling are not accessible (Rees 1986). Kashlinsky and Rees (1983) discussed fragmentation of primordial gas that cools via  $\text{H}_2$ . Couchman and Rees (1986) envisaged star cluster sized objects collapsing via  $\text{H}_2$  cooling at high redshift which then reionize the intergalactic medium. More recently, a model for the origin of halo globular clusters and spheroidal stars based on a cooling instability triggered by  $\text{H}_2$  formation has been put forward by Vietri and Pesce (1995). Furthermore, in studies of primordial star formation, molecular hydrogen cooling plays a central role (see Stahler 1986 for review). All these applications are of fundamental importance for our understanding of the origin of structure in the universe and its subsequent evolution.

All of the above problems are inherently multi-dimensional and a method that computes the hydrodynamics along with the chemistry is desirable. In order to form  $\text{H}_2$  efficiently through the above gas phase reactions, electrons and protons have to be abundant at relatively low temperatures ( $T < 10^4 \text{ K}$ ) allowing the formed molecules to survive. This situation arises naturally in shock heated gas, where the gas recombines slower than it can cool, and an enhanced ionized fraction (over the equilibrium value) is reached, despite the low temperatures.

This has been convincingly shown by many previous investigations (Hollenbach and McKee 1979, MacLow and Shull 1986, Shapiro and Kang 1987, Anninos and Norman 1996). Furthermore, at recombination the universe expands so fast that recombination will not be complete and the gas is left with a residual abundance of free electrons (see Peebles 1993). This residual ionized fraction can be enough to form a substantial amount of  $\text{H}_2$  in structures that only have very weak virialization shocks (see Couchman and Rees 1986; Tegmark *et al.* 1996). However, the chemistry has to be solved self-consistently with the structure formation equations, which is computationally due to the stiff nature of the reaction network. This has forced former studies to constrain themselves to zero dimensions, using e.g. steady state shock approximations. Only recently Haiman *et al.* presented a study of collapsing small scale structure that incorporated the time dependent chemistry in a one dimensional hydrodynamics code. In our methodology paper (Anninos, Zhang, Abel, & Norman 1996, hereafter AZAN96) we discuss a numerical method that unifies the time dependent chemistry with multi-dimensional cosmological hydrodynamics. With the chemistry model which accurately predicts abundances, and the cooling behaviour of primordial gas for temperatures from one to  $\sim 10^8$  Kelvin and all densities below  $\sim 10^4 \text{ cm}^{-3}$ , this introduces a powerful tool in investigating many aspect of structure formation by means of three dimensional hydrodynamical simulations.

The paper is organized in the following way: In the next section we review some general properties of primordial gas such as nucleosynthesis constraints and the coronal limit. In section 2.2. we discuss general arguments on how to select the dominant reactions. We then give an elaborate presentation of the collisional and radiative processes which we find to be important and the rate coefficients we have adopted. Section 5. gives an overview of the processes we find to be negligible for the range of applications we are interested in. Then we review all cooling mechanisms needed for our model and discuss the molecular cooling and heating functions in the low-density limit. Finally we present an extensive discussion of the performance of our model for an application to a strong shock wave arising from the collapse of a single pancake or cosmological sheet. The complete chemical model is summarized in appendix A.. The discussion why we find all  $\text{H}_2$  to be in its para configuration is given in appendix B..

## 2. General Properties of Primordial Gas

What are the major species determining the physics in primordial gas? Here we briefly summarize what we include in our cooling model and defer the detailed discussion to the following sections.

We know from nucleosynthesis and observational constraints that  ${}^7\text{Li}/\text{H} \sim 10^{-10}$ ,  $\text{D}/\text{H} \sim 10^{-5}$ ,  ${}^3\text{He}/\text{H} \sim 10^{-5}$ , and  $0.236 \leq {}^4\text{He}/\text{H} \leq 0.254$ . Where H, D, He, Li denote the mass abundances of hydrogen, deuterium, helium and lithium respectively. Hence D,  ${}^3\text{He}$ , and Li have, compared to neutral hydrogen, very low abundances. For the line cooling of D,  ${}^3\text{He}$ , and Li to contribute significantly to the overall cooling of the gas, their excitation rates would have to be many orders of magnitude higher than the corresponding processes of neutral hydrogen. However, this is not the case and those species, at least in their atomic and ionic forms, will have negligible influence on the hydrodynamics of the gas. The work by Lepp and Shull (1984) indicates that molecular hydrogen was by far the most abundant molecule in the universe at redshifts between recombination and before the first stars formed. It forms by radiative association of the negative hydrogen ion with neutral hydrogen and charge exchange between H and  $\text{H}_2^+$ . The minimal temperature at which rot./vib. of molecules can get excited defines a minimal temperature, and hence a minimal Jeans mass. In the case of molecular hydrogen, this introduces a minimum temperature of about  $10^2\text{K}$  (see also Mac Low and Shull 1986, Shapiro and Kang 1987) which translates to a Jeans mass of

$$M_J = \left( \frac{\pi k T}{\mu G} \right)^{\frac{3}{2}} \rho^{-\frac{1}{2}} \quad (5)$$

$$= 2 \times 10^5 M_\odot \left( \frac{T}{100\text{K}} \right)^{\frac{3}{2}} (n/\text{cm}^{-3})^{-\frac{1}{2}}, \quad (6)$$

which tells us that in an application as e.g. proto-galaxies, where we expect number densities of the order  $100\text{cm}^{-3}$  we expect a Jeans Mass of about  $10^4 M_\odot$ . This is a rough estimate of the minimum mass scale one has to resolve in numerical simulations. If one includes also HD and LiH which will get excited only for temperatures above 112K and 21K, respectively, one has to be able to resolve masses nearly a magnitude smaller. A study by D. Puy et al. (1993) was able to give fairly good estimates on the primordial HD abundance after recombination. They found that HD was the second most abundant molecule with  $n_{HD} \sim 10^{-3.5} n_{H_2}$ . We know, therefore, that molecular hydrogen will always be the dominant molecular coolant for temperatures above  $\sim 100\text{K}$ . Hence choosing to not include other molecules than  $H_2$  can be understood that we restrict our attention to masses greater than  $\sim 10^4 M_\odot (n/100\text{cm}^{-3})$ . Recently the Lithium Chemistry has been rigorously discussed by Stancil *et al.* 1996, where they found that much less primordial LiH is formed than previously expected and suggested that a significant fraction of LiH might only be formed by three body reactions. Since our model focuses at number densities below  $\sim 10^4 \text{cm}^{-3}$  and three-body reactions typically become important at greater densities we conclude that in the density regime we are interested in LiH will not be important. The papers mentioned above did not include  $H_3^+$  which, due to its low abundance is not believed to be a significant coolant. From the calculations by Lenzuni, Chernoff, and Salpeter (1991) we know that in fact the  $H_3^+$  abundance can be of the same order as the  $H_2^+$  abundance, but their results also show that it has a negligible effect on the molecular hydrogen abundance. We also did not include He molecular ions as well as hydrogen ion clusters ( $H_n^+$  with  $n \geq 4$ ) because their expected abundances are even smaller than the ones of the molecules mentioned above.

## 2.1. “Molecular” and “Atomic” Coronal Limit

Atoms and molecules have very complex intrinsic properties, and their chemical behavior varies sometimes drastically with the specific quantum-mechanical state they occupy. For atoms and ions at moderate or low densities like in the solar corona (electron number density  $n_e \sim 10^8 - 10^9 \text{cm}^{-3}$ ), the following features of thermodynamical equilibrium do *not* hold (Sobelman et al. 1979):

- Boltzmann distribution of atoms over excited states.
- Saha distribution of atoms over degrees of ionization.
- Principle of detailed balance.

The velocity distribution of the free electrons is, however, as a rule nearly always Maxwellian. In this low-density limit we know that the level distributions are given by,

$$\frac{N_i^k}{N_i^j} = n_e \frac{\langle v \sigma_{jk} \rangle}{A_k}$$

where  $N_i^k$  denotes the number density of the species  $i$  in its level  $k$ ,  $v \sigma_{jk}$  the rate coefficient for collisional excitation from level  $j$  up to level  $k$ ,  $A_k$  the total probability for spontaneous transition from all higher levels down to  $k$ . This approximation is applicable, if,

$$n_e \ll \frac{A_k}{\langle v \sigma_{jk} \rangle}$$

One important assumption here is that collisional excitations outweigh radiative excitations which is always true as long as there are only moderate external radiation fluxes. For the s-p excitation in Helium one finds

that the coronal limit holds up to electron densities of  $\sim 10^{17}\text{cm}^{-3}$ . ( Here we used  $\langle v\sigma_{jk} \rangle \sim 6 \times 10^{-9} \text{ cm}^3 \text{ s}^{-1}$  at 400K from Janev et al. 1987, (2.3.1), and  $A_k = 1.8 \times 10^9 \text{ s}^{-1}$  (Sobelman et al. 1979, p297)). Thus the coronal limit is valid for will be applicable in all our intended applications concerning structure formation. In proto-galactic clouds for example, we expect total number densities of about  $100 \text{ cm}^{-3}$ . For us the most important point is that we find nearly every atom in its ground state. Thus it is not necessary to treat multilevel atoms in our case.

Comparing the time scales for collisional excitation, collisional de-excitation (Lepp and Shull, 1983) and also the transition probabilities (Allison and Dalgarno, 1970) of molecular hydrogen, one finds that for low densities ( $n_H < 10^4\text{cm}^{-3}$  the population of excited states of  $\text{H}_2$  is by many orders of magnitude smaller, than the ground state. This is a fact which can also be seen in Lepp and Shull 1983, as well as in the work of Dove et al. 1987 where they studied dissociation of molecular para-hydrogen by collisions with helium. They found that at low densities the dissociation rate coefficient approaches a constant value, which corresponds to direct collisional dissociation out of the ( $v = 0, J = 0$ ) level only. A strong radiation field in the UV is capable of populating the exciting states and hence changing the chemical behaviour of  $\text{H}_2$ . However, a detailed study (Shull 1978) shows that only for fluxes greater than  $\sim 5 \times 10^{-15} \text{ erg cm}^{-2} \text{ s}^{-1} \text{ Hz}^{-1} \text{ sr}^{-1}$  UV Pumping becomes effective. We conclude that in our intended calculations we can assume all our considered species to be in their ground state.

## 2.2. Selection of Reactions and Rate Coefficients

Although primordial gas is a simple mixture of hydrogen and helium, the ongoing physical reactions in it are immense. E.g. in Janev *et al.* 1987 one finds more than 70 reactions only involving the ground states of our species. It is obvious that in order to construct a computationally feasible model that some selections have to be made. The quest is to make them as good as possible i.e. without neglecting any important physics. To neglect a collisional processes one, obviously, has to make sure that

1. for all reactants and products the rate will for any temperature and density never dominate the right hand side of the rate equations.
2. the reaction enthalpy is always negligible energy contribution or loss to the internal energy of the gas.

We used these criteria to construct our reaction network out of hundreds of reactions found in the literature as well as in databases.

## 3. Collisional Processes

In appendix A., we present all included processes, their rate coefficients and the according reference. Discussing the reliability of the used rate coefficients and their sources will be the main aim of this section. Further information on atomic rates can be found at **Dima Verners 1996 Atomic Data Page** (<http://www.pa.uky.edu/verner/atom.html>)

### 3.1. Ionizing processes

For the cosmological problems we are interested in, we have seen above that spontaneous decay is a lot faster than collisional excitation (coronal limit). This already pointed out the non-LTE character of our problem. Metaphorically speaking, the radiation field is in our case much smaller than in the LTE case, since there are

not enough collisional excitations to build up a Planckian spectrum. Therefore, if we compare in the following collisional and radiative processes, we can use arguments derived for strict LTE for qualitative statements on non-LTE conditions by assuming that the radiation temperature is much less than the matter temperature. This is always true in the matter dominated phase of the universe, when radiation fields other than the CBR are negligible. We adopt here Mihalas' (1978, p123) estimate of the ratio between the total number of photoionizations  $R_{ik}$  and the total number of collisional ionizations  $C_{ik}$ ,

$$\frac{R_{ik}}{C_{ik}} \approx \frac{4(2\pi^3)^{\frac{1}{2}} E_i^3}{3m^{\frac{1}{2}} e^2 h^2 c^3} \left( \frac{W k_B T_R}{n_e (k_B T_e)^{\frac{1}{2}}} \right) \exp \left[ h\nu_0 \left( \frac{1}{k_B T_e} - \frac{1}{k_B T_R} \right) \right],$$

where  $E_i$  is the ionization energy out of the level  $i$ ,  $k_B$  is the Boltzmann constant,  $m$  is the electron mass,  $T_e$  the electron temperature,  $e$  the electron charge,  $c$  the speed of light, and  $W$  is defined by  $J_\nu = W B_\nu(T_R)$ , where  $J_\nu$  is the specific intensity at the frequency  $\nu$ , and  $B_\nu(T_R)$  denotes the Planck spectrum of a black body with temperature,  $T_R$ .

This gives for ionization of hydrogen out of the ground state ( $E_i = 13.6\text{eV}$ ) with the number density of free electrons in  $\text{cm}^{-3}$ ,

$$\frac{R_{ik}}{C_{ik}} \approx 1.55 \times 10^{14} \frac{W}{n_e} \left( \frac{T_R^2}{T_e} \right)^{\frac{1}{2}} e^{157820 \left( \frac{1}{T_e} - \frac{1}{T_R} \right)}$$

In thermal equilibrium with  $T_e = T_R \sim 10^4$  and  $n_e \sim 1\text{cm}^{-3}$  this ratio is of the order  $10^{15}$ , therefore radiative ionization dominates by far. For  $T_e \sim 10 \times T_R \sim 10^3$ , however, the ratio  $\frac{R_{ik}}{C_{ik}}$  is of the order  $10^{-47}$  and we see that for all of our intended applications collisional ionization is the dominating process. It is important, however, to include photoionization to study the influence of external radiation fields on the chemistry and the cooling to heating balance of the structure forming gas, as, e.g., Lyman Alpha clouds in the vicinity of quasars which are observationally accessible.

**(1) Collisional Ionization of Hydrogen** We use the fit of Janev et al. (1987, 2.1.5). For temperatures below  $1000\text{K} \sim 0.086\text{eV}$  we take it to be zero since it is smaller than  $10^{-60}\text{cm}^3\text{s}^{-1}$ . Since in our simulations we do not expect to encounter temperatures above  $10^5\text{eV}$  no relativistic corrections were made. The ionization threshold is  $13.6\text{eV}$ .

**(2) Collisional Ionization of Helium** We use the fit given by Janev et al. (1987, 2.3.9) For temperatures below  $4000\text{K}$  we take it to be zero since it is smaller than  $10^{-38}\text{cm}^3\text{s}^{-1}$ . The threshold lies at  $24.6\text{eV}$ .

**(3) Collisional Ionization of He<sup>+</sup>** The rate is given in the Aladdin Database (1989) of the IEADS (International Atomic Energy Agency, Data Section). The energy threshold is  $54.4\text{eV}$ . Again we only have to consider ionization out of the ground state and no relativistic effects.

### 3.2. Radiative Recombination

Radiative recombination is the inverse reaction of photoionization. With a similar argument as the one we used to discuss the relative importance of collisional to radiative ionization, one finds (Mihalas 1978) that radiative recombination always outweighs the collisional one. This is especially valid in our low-density limit since the collisional recombination which is, as all three-body processes, typically negligible for densities smaller than about  $10^8\text{cm}^{-3}$ .

**(4) Radiative Recombination to Hydrogen** In the coronal limit we assume that recombination can happen into any quantum state which, if it is an excited state, will spontaneously decay to the ground state. Therefore, the total rate coefficient is the sum of the rate coefficients  $\alpha_n$  for all  $n = 1..∞$ . Ferland et al. (1992) computed hydrogenic rate coefficients which are in principle exact. We have fitted their data (the sum of all rate coefficients for  $n = 1..1000$ ) to a form similar to what Janev et al. (1987) used in their compendium. We made sure that the fit is accurate for temperatures from 1K to  $10^9$ K.

**(5, 6) Recombination to Helium**  $\text{He}^+$  is the only species in our model, which is subject to di-electronic recombination which dominates at high temperatures ( $T > 6 \times 10^4$ K). Since radiative and di-electronic recombination rates are independent of density their sum gives the overall recombination rate. For the radiative recombination process we employ the rate coefficient given by Cen (1992) and for the di-electronic recombination the one given by Aldrovandi & Pequignot (1973).

**(7) Photo-attachment of Hydrogen** The rate coefficient from Hutchins (1976) is stated to be accurate to 10% in the temperature range  $100\text{K}(= 0.0086\text{eV}) \leq T \leq 2500\text{K}(= 0.254\text{eV})$ . The cross section for the inverse reaction has been calculated by Wishart (1979) to within 1% around the threshold ( $2 \times 10^{14}\text{Hz} < \nu < 2 \times 10^{15}\text{Hz}$ ). From that data alone one can compute the rate for photo-attachment from 2000K to 10000K, using the principle of detailed balance or simply the Saha equation. To cover a greater temperature range, however, we use the cross section given in de Jong (1972) for all frequencies outside of the interval given by Wishart (1979). With that we are able to compute and fit this rate in the temperature range from 1K to  $10^8$ K, with an accuracy to within a few percent for  $1\text{K} < T < 100\text{K}$ , about one percent for  $100\text{K} < T < 10^4\text{K}$ , and better than 10% for  $T > 10^4\text{K}$ . At LTE the Saha equation has to be valid and the rate at non-LTE will be naturally the same as in LTE since it is an atomic property. The Saha-Boltzmann ionization equation reads,

$$\frac{k_{det}}{k_{att}} = \frac{N_{r+1}}{N_r} N_e = \frac{u_{r+1}}{u_r} \frac{2(2\pi m k T)^{3/2}}{h^3} \exp\left(-\frac{I_r}{kT}\right),$$

where  $N_e$  denotes the free electron number density,  $N_{r+1}$  the number density of neutral hydrogen atoms,  $N_r$  the number density of  $\text{H}^-$  ions,  $k_{det}$  the rate coefficient for photo-detachment,  $k_{att}$  the rate coefficient for photo-attachment,  $u_r, u_{r+1}$  the respective partition functions,  $I_r$  the threshold for photo-detachment of  $\text{H}^-$  (0.755eV),  $m$  the electron mass, and  $k$  the Boltzmann constant. The single bound state of  $\text{H}^-$  is  $^1\text{S}$  and the ground state of  $\text{H}$  is  $^2\text{S}$ . Hence  $u_{r+1} = 2$  and  $u_r = 1$ . The rate coefficient,  $k_{det}$ , for photo-attachment in LTE is derived by integrating the cross section over a Planckian black body spectrum. The fit, which is given in the appendix, equals the one given by Hutchins (1976) to within a few percent in the range where the latter is applicable.

**(8) Formation of molecular Hydrogen via  $\text{H}^-$**  The rate coefficient has been taken from Janev et al. (1987, 7.3.2.b) and is based on theoretical cross sections of Browne and Dalgarno (1969) and normalized to the experimental results of Hummer et al. (1960) in the region of 500eV to  $4 \times 10^4$ eV. We averaged their energy dependent rate coefficient over a Maxwellian velocity distribution of the incident particle. The used data is only reliable for temperatures above 0.1eV. However, we, know that the rate coefficient is constant for small temperatures and we also see that the energy dependent rate coefficient is already the same for 0.1eV and 1eV of the incident particle for a temperature of 0.1eV. Therefore, we take the rate coefficient at 0.01eV to be the same as at 0.1eV, fit it, and set it to be constant for lower values. This leads to a value of the rate coefficient for low temperatures about 10% higher than the constant values given by Bieniek (1980) and de Jong (1972). Launay, Le Dourneuf, and Zeippen (1991) computed the ratecoefficient for this reaction depending on the ro-vibrational state of the produced  $\text{H}_2$  molecule. Using the potential derived by Senekowitsch *et al.* they found a thermal rate at 300 K of  $1.49 \times 10^{-9}$  which lies 4% above the rate we derived from the data of Janev et al. (1987).

**(9) Formation of  $\text{H}_2^+$**  The rate coefficient for this radiative association reaction has been calculated by Ramaker and Peek (1976) and has then been fitted by Shapiro and Kang (1987) as well as by Rawlings et al. (1993). We prefer the fit given by Shapiro and Kang, because it covers a greater temperature interval.

**(10)  $\text{H}_2$  Formation via  $\text{H}_2^+$**  The rate constant for this charge exchange reaction between neutral hydrogen and  $\text{H}_2^+$  was measured by Karpas et al. (1979) to an accuracy better than 20%. This rate is constant at low energies because the distribution of final states in phase space is determined by the energy released in the reaction, which is almost independent of the incident energy (Peebles 1993). By assuming it to be constant at high temperatures as well, we potentially introduce an error in the  $\text{H}_2$  abundance, because the by far dominating destroying processes will be balanced by a wrong formation rate. However, this error will not be significant because the formation of hydrogen molecules is dominated by the  $\text{H}^-$  formation path. Figure 1 summarizes the rate coefficients for formation of  $\text{H}^-$  and  $\text{H}_2^+$  as well as the ones for  $\text{H}_2$ .

**(11) Charge Exchange between Molecular Hydrogen and  $\text{H}^+$**  This is the inverse reaction of the above. The rate coefficient was derived by Donahue and Shull using detailed balance and the Karpas et al. (1979) data to

$$k_{11} = 6.4 \times 10^{-10} \exp\left(-\frac{2.65\text{eV}}{T_{eV}}\right).$$

That rate differs drastically from the one we have computed from data given in Janev et al. (1987) which is accurate also for high temperatures. The data of Janev *et al.* has to be considered by far more accurate than the simple detailed balance argument of Donahue and Shull (1991). However, comparing results of our model with the one of Shapiro and Kang (1987) we find that drastic differences in this rate do not change the final abundances significantly.

**(12) Dissociation of molecular Hydrogen by Electrons** We employ the rate coefficient that Donahue and Shull (1991) derived from the cross section given by Corrigan (1965).

**(13) Dissociation of Molecular Hydrogen by neutral Hydrogen** Dove and Mandy used fully 3D quasi-classical trajectory calculations, using the Siegbahn-Liu-Truhlar-Horowitz potential energy surface, to calculate the rate coefficient in the low density limit. They found significant differences to the former “standard” values given by Lepp and Shull (1983). We use the results for the total rate coefficient of Dove and Mandy (1986), which assumes that all the quasi-bound states will dissociate. Although their ratecoefficient is not accurate at temperatures well below 500 K this does not lead to a significant error in the  $\text{H}_2$  abundance as can clearly be seen from the discussion in section 7.1.

**(14) Collisional Detachment of  $\text{H}^-$  by Electrons** We take the rate coefficient from Janev et al. 1987 (7.1.1), which is based on experimental results. The net energy loss is as in ionization reactions the threshold energy which is 0.755eV.

**(15) Collisional Electron Detachment of  $\text{H}^-$  by neutral Hydrogen** The formation of an auto-dissociating state of molecular hydrogen, (equation 13 in section 5.6.) seems to be far more effective in destroying  $\text{H}^-$  than the direct collisional detachment



The rate coefficient for the auto-dissociating state below 0.1eV is very uncertain. We have extrapolated the data given by Janev et al. (1987) linearly for those temperatures. This overestimates the rate coefficient in



this range. However, it does not introduce any significant error in the abundances since for a collision of  $\text{H}^-$  with  $\text{H}$  in this temperature regime it is far more probable to form a stable  $\text{H}_2$  molecule than to destroy the  $\text{H}^-$ . In fact, we expect this reaction to be only of importance in a very small range around 1eV, since for higher temperatures, the dissociation by free electrons is far more effective than the one by  $\text{H}$ .

**(16) Mutual Neutralization between  $\text{H}^-$  and  $\text{H}^+$**  The rate coefficient given by Dalgarno and Lepp (1987) is consistent with the measurements by Szucs *et al.* (1984) and Peart, Bennett and Dolder (1985). See the latter reference for a review on the experimental difficulties and uncertainties of ion-ion collisions.

**(17)  $\text{H}_2^+$  Formation in  $\text{H}^-$  and  $\text{H}^+$  Collision** Shapiro and Kang (1987) derived the rate coefficient from the cross section which was measured by Poulaert *et al.* (1978) in the range from 0.001eV to 3eV and found to have a  $E^{-0.9}$  dependence with  $1.5 \times 10^{-14} \text{cm}^2$  at 0.003eV. The fit given in Shapiro and Kangs (1987), however, is discontinuous at  $10^4 \text{K}$ . We changed it within 4%, which surely lies within the uncertainties of the experimental data to make it continuous. The result is given in the appendix.

**(18) Dissociative Recombination of  $\text{H}_2^+$  with slow Electrons** The rate for this reaction was calculated using multichannel quantum defect theory (MQDT) by Nakashima *et al.* (1987) in the energy range from 0.02 to about 1eV. Their result is much smaller at low temperatures, than previously assumed (see e.g. Shapiro and Kang 1987, Mitchell and Deveau 1983). More recently Schneider *et al.* (1994) recalculated this rate coefficient also using MQDT. Their tabulated rate coefficient for dissociative recombination of the  $\text{H}_2^+$  ground state via the  $\Sigma_g^+$  state is, above 1000K, by a factor of two to four smaller than the rough fit given by Nakashima. Our fit of the Schneider *et al.* (1994) data neglects the fact that the rate is increasing for  $T < 50 \text{K}$ . This is reasonable since one does not expect this reaction to be important for temperatures smaller than 100K due the small abundance of free electrons, as well as  $\text{H}_2^+$ .

**(19) Neutralization between  $\text{H}_2^+$  and  $\text{H}^-$**  This mutual neutralization reaction takes place at low energies ( $< 1 \text{eV}$ ) where  $\text{H}_2^+$  and  $\text{H}^-$  coexist. Unfortunately, the only three measurements we are aware of, Aberth *et al.* in Moseley *et al.* (1975), Szucs *et al.* (1983), and Dolder & Peart (1985), give only data for energies above 3eV. We use the rate coefficient given by Dalgarno and Lepp (1987) despite its uncertainty. This equals the coefficient given by Prasad and Huntress (1980) which was used by Shapiro and Kang (1987) to within 25%.

#### 4. Photoionization and Dissociation Processes

In general we will only consider photoionization (dissociation) out of the ground state since we assume the abundance of excited states to be negligible. The rate of a particular photoionization (dissociation) reaction is given by:

$$\frac{\partial \rho_k}{\partial t} / \rho_k = \int_{\nu_{th}}^{\infty} 4\pi \sigma_{\nu}^k \frac{i(\nu)}{h\nu} d\nu, \quad (7)$$

where  $k$  denotes  $\text{H}$ ,  $\text{He}^+$ ,  $\text{H}^-$ ,  $\text{H}_2^+$  and  $\text{H}_2$  respectively,  $i(\nu)$  is the intensity of the radiation field,  $\nu_{th}$  the threshold energy for which photo ionization(dissociation) is possible, and  $\sigma_{\nu}^k$  the frequency dependent photoionization (dissociation) cross section of species  $k$ .

**(20 – 22) Photoionization of H, He and He<sup>+</sup>** Hydrogenic cross sections have been studied in great detail. Since they are relatively simple to calculate the available data is very accurate. We use the typical expression given in Osterbrook (1989). The threshold frequencies are  $h\nu = 13.6\text{eV}$ ,  $24.6\text{eV}$ , and  $54.4\text{eV}$ , for H, He, and He<sup>+</sup>, respectively.

**(23) Photo-detachment of the H<sup>-</sup> Ion** The best data available is given by Wishart (1979) with a stated accuracy within 1%. The fitting formula for the cross section given in Shapiro and Kang (1987) is accurate to  $\sim 10\%$  at the high energy end. This is a normal characteristic of such fitting formulas. Although is adequate for present purposes, we recommend using the tabulated values of Wishart (1979), where they are available, in order to derive the rate of H<sup>-</sup> destruction since using the fitting formula in the integral of equ. 7 leads to an overestimation of the according rate. H<sup>-</sup> gets destroyed efficiently by the CBR to redshifts  $\sim 110$ . A fit for  $k_{23}$  depending on radiation temperature can be found in Tegmark *et al.* 1996 (<http://www.mpa-garching.mpg.de/max/minmass.html>).

**(24) Photoionization of Molecular Hydrogen** The high threshold of  $15.42\text{eV}$  assures that the CBR will not be able to photo-ionize H<sub>2</sub> in the post-recombination universe. The rate is taken from Shapiro and Kang (1987).

**(25 – 26) Photodissociation of H<sub>2</sub><sup>+</sup>**

There is a conceptual difficulty in the treatment of this process since for strong radiation fields and high densities, excited states of H<sub>2</sub><sup>+</sup> will be populated. For them the photodissociation cross sections are much higher than for the ground state. However, the levels might not be in their thermal equilibrium distribution. To treat this exact, one would have to include all H<sub>2</sub><sup>+</sup> levels explicitly, which for our applications would not be worth the effort since most of the H<sub>2</sub> is formed via H<sup>-</sup>. By using solely the cross section for the ground state we will overestimate the H<sub>2</sub><sup>+</sup> abundance. Using the LTE rate one could derive a lower limit and estimate the error made, which we did not attempt in our simulations, yet. The most recent data for dissociation out of the ground state as well as LTE rates can be found in Stancil (1994). We have fitted the cross section for the ground state to better than 2%. This fit is more accurate, and also does not show the unfortunate divergent character than the one given in Shapiro and Kang (1987) which was drawn from Dunn (1968). The threshold energy is  $2.65\text{eV}$ . For photons with energies greater than  $30\text{eV}$ , H<sub>2</sub><sup>+</sup> can get dissociated with two protons as products (proc. 26). For this we adopted the rate given in Shapiro and Kang (1987).

**(27) Photodissociation of H<sub>2</sub> by predissociation** Photodissociation of the ground state of molecular hydrogen ( $X^1\Sigma_g^+(v)$ ) happens mostly through absorption in the Lyman-Werner Bands to the electronically and vibrationally excited states,  $B^1\Sigma_u^+(v')$  and  $C^1\Pi_u(v')$  which then decay to the continuum of the ground state. This is called the two-step Solomon process (cf. Stecher and Williams, 1967). Allison and Dalgarno (1970) computed the band oscillator strengths and Dalgarno and Stephens (1970) derived the probability that those states decay into the continuum of the ground state. The dominant photodissociation paths are through absorption in the Lyman Band to the vibrational states  $6 < v' < 20$ . This means that H<sub>2</sub> dissociation happens mostly in a very narrow frequency range  $12.24\text{eV} < h\nu < 13.51\text{eV}$ . Assuming the incident radiation field to be practically constant around  $h\bar{\nu} = 12.87\text{eV}$ , which corresponds to  $v' = 13$ , and neglecting self-shielding we can derive a rate constant for photodissociation of H<sub>2</sub> through

$$\begin{aligned}
 k_{27} &= \sum_{v'} \frac{\pi e^2}{mc} f_0^{v'} p_{Ly}^{v'} \int \frac{j(\nu)}{h\nu} \phi_{v'}(\nu) d\nu \approx \frac{j(\bar{\nu})}{h\bar{\nu}} \sum_{v'} \frac{\pi e^2}{mc} f_0^{v'} p_{Ly}^{v'} \\
 &\sim 1.1 \times 10^8 \frac{j(\bar{\nu})}{\text{ergsHz}^{-1}\text{s}^{-1}\text{cm}^{-2}} \text{ s}^{-1},
 \end{aligned}$$

where  $j$  denotes the radiation flux in  $\text{s}^{-1}\text{ergs cm}^{-2}\text{Hz}^{-1}$  at  $h\nu = 12.87\text{eV}$ ,  $f_0^{v'}$  the oscillator strength for the transition  $X^1\Sigma_g^+(v=0)$  to  $B^1\Sigma_u^+(v')$ ,  $p_{Ly}^{v'}$  the probability that  $B^1\Sigma_u^+(v')$  decays to the continuum,  $\phi_{v'}(\nu)$  the line profile, and  $\pi e^2/(mc) = 2.65 \times 10^{-2}\text{cm}^2$  the classical total cross section.

**(28) Direct Photodissociation of H<sub>2</sub>** Direct photodissociation of the ground state by absorption into the continua of the Lyman and Werner systems has been studied by Allison and Dalgarno 1969. We have fitted their cross sections within the stated accuracy of their data with,

$$\sigma_{28} = \frac{1}{y+1}(\sigma_{28}^{L0} + \sigma_{28}^{W0}) + (1 - \frac{1}{y+1})(\sigma_{28}^{L1} + \sigma_{28}^{W1}) \quad (8)$$

where

$$\sigma_{28}^{L0} = 10^{-18} \times \begin{cases} \text{dex}(15.1289 - 1.05139 \times h\nu) \text{ cm}^2, & 14.675 \text{ eV} < h\nu < 16.820 \text{ eV} \\ \text{dex}(-31.41 + 1.8042 \times 10^{-2}(h\nu)^3 - 4.2339 \times 10^{-5}(h\nu)^5) \text{ cm}^2, & 16.820 \text{ eV} < h\nu < 17.6 \text{ eV}, \end{cases} \quad (9)$$

$$\sigma_{28}^{W0} = 10^{-18} \times \begin{cases} \text{dex}(13.5311 - 0.9182618h\nu) \text{ cm}^2, & 14.675 \text{ eV} < h\nu < 17.7 \text{ eV}, \end{cases} \quad (10)$$

$$\sigma_{28}^{L1} = 10^{-18} \times \begin{cases} \text{dex}(12.0218406 - 0.819429h\nu) \text{ cm}^2, & 14.159 \text{ eV} < h\nu < 15.302 \text{ eV}, \\ \text{dex}(16.04644 - 1.082438h\nu) \text{ cm}^2, & 15.302 \text{ eV} < h\nu < 17.2 \text{ eV}, \end{cases} \quad (11)$$

$$\sigma_{28}^{W1} = 10^{-18} \times \begin{cases} \text{dex}(12.87367 - 0.85088597h\nu) \text{ cm}^2, & 14.159 \text{ eV} < h\nu < 17.2 \text{ eV}, \end{cases} \quad (12)$$

and  $y$  is the ortho-, to para-H<sub>2</sub> ratio. Since unfortunately they only gave the data for photon excess energies up to 3 eV one might make quite significant errors in deriving the ratecoefficient where one integrates over this cross section. The error made depends on the shape of the radiation spectrum.

## 5. Brief Summary of Neglected Processes

In this section we will briefly summarize some processes which we find to be negligible. Although we can almost be sure that this summary will be far from complete, we hope to stimulate with this a discussion which should lead us to a more detailed understanding of the primordial gas chemistry and enable us to find the minimum set of reactions, which describes primordial gas accurately enough for the desired cosmological applications.

### 5.1. Photoionization Heating and Secondary Ionization

For all simulations where we do want to consider strong external radiation fluxes we have to look at the fate of the photo electrons produced in photoionizations. To estimate the importance of this effect we first derive the numbers of high energy photo electrons produced in a typical quasar radiation field.

Shapiro and Kang (1987) modeled a quasar radiation flux with:

$$F_\nu = 1.0 \times 10^{-21} \epsilon \left( \frac{\nu}{\nu_H} \right)^{-\alpha} \text{ ergs cm}^{-2} \text{ s}^{-1} \text{ Hz}^{-1},$$

where  $\nu_H$  is the Lyman edge frequency,  $\alpha = 0.7$ ,  $0.7\text{eV} < h\nu \leq 12.4\text{keV}$ , and  $\epsilon$  is a parameter introduced to adjust the amplitude of the flux (or effectively the distance of the quasar). Although Sargent, Steidel, and Boksenberg (1989) argued that  $\alpha \geq 1$  might be a better fit, we will derive an upper limit of produced photo

electrons with the more drastic value of  $\alpha = 0.7$ . We calculated the fraction  $n_{\gamma, e^-}^{low}/n_{\gamma, e^-}^{high}$  between the electrons produced by photons in the range from  $h\nu_H$  to  $2h\nu_H$  and the ones produced by photons in the range of  $2h\nu_H$  to  $12.4\text{keV}$ :

$$\frac{n_{\gamma, e^-}^{low}}{n_{\gamma, e^-}^{high}} = \frac{\int_{\nu_H}^{2\nu_H} F_\nu \frac{\sigma_{20}(\nu)}{h\nu} d\nu}{\int_{2\nu_H}^{24\text{keV}/h} F_\nu \frac{\sigma_{20}(\nu)}{h\nu} d\nu}.$$

For a very hard spectrum with  $\alpha = 0.7$  we get  $n_{\gamma, e^-}^{low}/n_{\gamma, e^-}^{high} = 10$  whereas for a more soft spectrum this number increases (e.g. 13 for  $\alpha = 1.0$ ). Because photo electrons have an energy of  $h(\nu - \nu_H)$ , the ones produced by photons in the range from  $h\nu_H$  to  $2h\nu_H$  will not be capable of collisionally ionizing any species other than  $\text{H}^-$ . Therefore, all they can do is to either go into heat, which means scatter with other electrons or ions and equilibrate to a Maxwellian distribution, or excite other atoms, ions or molecules. The photo electrons above  $2h\nu_H$  carry enough energy to also ionize (dissociate) other species. The very high energetic ones are capable of ionizing (dissociating) many atoms (molecules) while cooling down. Shull and van Steenberg (1985) gave fits for the fraction of photo electrons above 100eV which go into heat, ionization, and excitation respectively. We however find that the total energy of all photo electrons above 100eV is only 1.5% of the total energy of all the photo electrons produced in photoionization of neutral hydrogen by a typical quasar flux. Hence we do not believe those photo electrons to be significant. The ones in the range of  $h\nu_{th}$  to 100eV make up about one third of all of the produced photo electrons. Fig.3 of Shull and Van Steenberg (1985) shows that even for a mostly neutral gas, maximally about 30% secondary electrons will go into ionization. We conclude that by leaving out secondary ionization we will make an error in the estimates of the ionized fraction of always less than 10%.

The estimates above were based on the photoionization cross section of hydrogen, but they hold in general for the following reasons. First, the cross sections for He and  $\text{He}^+$  scale as  $\nu^{-3}$  in the high frequency limit, and second, nucleosynthesis predicts  $n_H \sim 16n_{He}$ . Therefore the photo electrons produced in photoionizations of neutral hydrogen are the dominant ones. Clearly, the above discussion only justifies the approximation of leaving out the effects of photo electrons, for applications where the radiation spectrum is approximated well by a power law as given in equ. 5.1..

## 5.2. Exciting Collisions

For our intended low density applications the coronal limit (see above) holds and we therefore know that any excitation of H,  $\text{H}^-$ , He,  $\text{He}^+$ , and  $\text{H}_2$  will be followed by a spontaneous decay back into the ground state and so ensure that practically every atom or ion will be in its ground state most of the time. An excitation does not change the abundance of our model species and does not enter the reaction network explicitly. We, however, will consider the dominant ones in the energy balance through appropriate cooling functions.

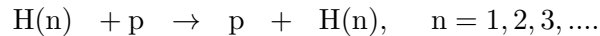
## 5.3. Collisions of Electrons with Atoms and Ions

Electrons can photo-attach with, ionize, and excite, neutral hydrogen and helium and also ionize, recombine with, and excite their ions. We included all radiative recombination and collisional ionization reactions (procs. 1–6, 14) except the double ionization of helium since it does not significantly influence the ionization balance due to its high threshold. The dominant excitations (see above) are treated through the appropriate cooling functions. We also included the photo-attachment reaction of neutral hydrogen (proc. 7). No reference for photo-attachment of neutral helium could be found but one can be confident that its effects are by far dominated by  $\text{H}^-$  which is the main species for the formation of molecular hydrogen and thereby controlling the cooling of primordial gas at low temperatures.

#### 5.4. Proton Collisions with Neutral Helium and Hydrogen

Below temperatures of  $\sim 1\text{eV}$  the neutral atoms are the most abundant species, whereas free protons and  $\text{He}^+$  are, even in the non-equilibrium case, more than two orders of magnitude less abundant than H, and He respectively (Shapiro and Kang 1987). For the equilibrium case this difference is far more drastic.

We checked all proton collisions listed in Janev et al. 1987 and find that the rate coefficients typically drop drastically for temperatures below 10eV. This is especially true for collisional ionization by protons. The exception to the rule are charge exchange reactions as,



Since we expect nearly all hydrogen atoms to be in the ground state, the  $n = 1$  case will be the most probable process. Although it does not enter the reaction network, since it “produces what it destroys”, it is an important reaction theoretically since it ensures tight thermal and spatial coupling between the protons and the ions due to its relatively high rate coefficient of  $\sim 10^{-8} \text{ cm}^3 \text{ s}^{-1}$ .

All rate coefficients for the excitation of neutral hydrogen and helium by protons out of the ground state are smaller by many orders of magnitude than the one for excitation by electrons. Since charge neutrality requires that there are about as many free electrons as protons, we know that excitation by electrons dominates excitations by protons.

#### 5.5. Collisions of Hydrogen with Helium and their Ions

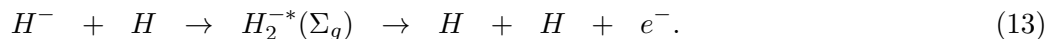
An interesting feature of the presented reaction network is that all species which are build up by hydrogen nuclei couple with the species formed by helium nuclei only by the free electron fraction. This is due to the following reasons;

1. Electrons are much more effective in ionizing than any other species since their mean velocity is  $(Am_H/m_e)^{1/2} \approx 43A^{1/2}$  times higher than for an ion with  $A$  times the proton mass.
2. Charge Exchange between H and  $\text{He}^+$  has a rate coefficient  $\sim 1.9 \times 10^{-15} \text{ cm}^3 \text{ s}^{-1}$  and is according to Couchman (1985) negligible.
3.  $\text{H}^-$ ,  $\text{H}_2^+$ , and  $\text{H}_2$  are not capable of ionizing helium. They are relatively fragile and have very small abundances at temperatures above  $\sim 1\text{eV}$  where they have kinetic energies far below ionization thresholds.

A discussion why the reaction network does not include processes where helium or its ions destroy  $\text{H}^-$ ,  $\text{H}_2^+$ , or  $\text{H}_2$  can be found in the subsequent sections.

#### 5.6. Neglected Dissociating Reactions of $\text{H}^-$

Electron detachment of  $\text{H}^-$  through neutral helium has according to the ALADDIN database of the IAEADS, a cross section of the order  $\sim 10^{-16} \text{ cm}^2$  and is therefore by many orders smaller than the cross section ( $\sim 10^{-9} - 10^{-7} \text{ cm}^2$ ; Janev et al. 1987, 7.3.2a) of reaction



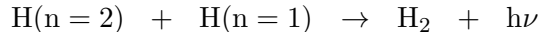
Exactly the same argument holds for electron detachment of  $\text{H}^-$  through molecular hydrogen which has a cross section  $\sim 10^{-18} - 10^{-16} \text{ cm}^2$  (ALADDIN database).

We did not include mutual neutralization of  $\text{H}^-$  with  $\text{He}^+$ . The available data from the IAEADS via the ALADDIN database, which is only valid for energies above 42eV, indicates that the cross section of mutual neutralization of  $\text{H}^-$  with  $\text{He}^+$  is higher than for mutual neutralization with protons. That is what one might naively expect when considering that the Coulomb attraction, acts as the driving force for this reaction, competing with the kinetic motion of the reactants. Since  $\text{He}^+$  is heavier than H its mean velocity will be slower but the Coulomb attraction is the same therefore mutual neutralization with  $\text{He}^+$  should occur with a higher rate. We only leave out this reaction due to the lack of reliable data. However, the expected error is small since at low temperatures most of the  $\text{H}^-$  will react with neutral hydrogen and form molecular hydrogen (proc. 7) and at higher temperatures ( $>8,000\text{K}$ ) collisional detachment by free electrons (proc. 14) will dominate the destruction of  $\text{H}^-$ .

Neutralization between  $\text{H}^-$  and  $\text{He}^{++}$  can be neglected due to the high temperature threshold for  $\text{He}^{++}$  formation. Whenever  $\text{He}^{++}$  is formed the temperature is so high that nearly all  $\text{H}^-$  will be destroyed.

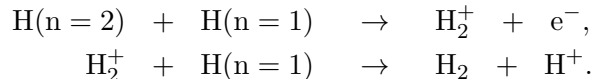
### 5.7. Omitted reactions for $\text{H}_2$ formation

Molecular hydrogen formation by excited atom radiative association



has a very small rate coefficient, due to the zero dipole moment of molecular hydrogen (Latter and Black 1991). Also, for the cosmological applications we are interested in, the  $n=2$  population is extremely small in all cosmological applications making this process less significant than the dominant  $\text{H}_2$  formation mechanisms (procs. 8,10).

We also neglect the formation path where  $\text{H}_2^+$  first gets formed by excited atom radiative association and then forms molecular hydrogen through the charge exchange with neutral hydrogen (proc.10) (Rawlings *et al.* 1993).

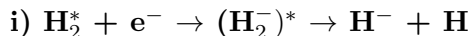


This process can in certain circumstances, e.g. dense and hot gas in circumstellar environment, dominate formation by excited atom radiative association. In our intended cosmological applications these processes, however, will never be significant, since the population of excited states is always negligible.

### 5.8. Collisional Dissociation of $\text{H}_2$ and $\text{H}_2^+$

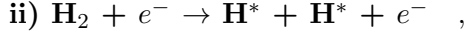
Since the hydrogen molecule is the main coolant for gas at temperatures below  $\sim 1\text{eV}$  we pay special attention to its destruction mechanisms. We follow here Shapiro and Kang (1987) and assume that at every dissociation 4.476eV are lost. In the following we will discuss dissociating reactions which we find to be negligible compared to the three dissociating reactions we have included in our model and which are illustrated in Figure 2.

#### 5.8.1. Dissociation of molecular Hydrogen by $e^-$



Wadehra and Bardsley (1978) showed that this dissociative attachment reaction depends strongly on the vibrational and rotational states. For low density gas ( $n_H < 10^5\text{cm}^{-3}$ ) in which nearly all hydrogen molecules

will be in their ground state its rate is of the order  $10^{-15}\text{cm}^3\text{s}^{-1}$  for an electron temperature of 1eV. For electron temperatures below that this rate drops drastically even further. After comparing this to Figure 2 we conclude that this process will never play an important role for the destruction of  $\text{H}_2$  in our applications. It is, however, a crucial process in situations with either densities above  $10^4\text{cm}^{-3}$  or intense ultraviolet radiation fluxes, because under those circumstances the excited states will become populated (for vibrational excitation of molecular hydrogen in intense UV fluxes see Shull 1978).



Our process 12 is,

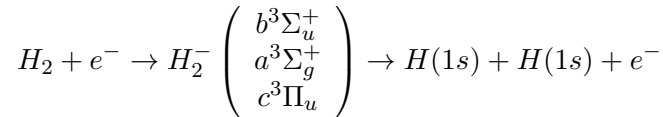


and dominates all other reactions of the type,



Intuitively one would have expected this because in proc. 15 the incident energy has to be enough to excite the produced H atoms. However, the  $2s$  level already lies 10.2eV above the ground state which only few electrons have at the low temperature ( $< 1\text{eV}$ ) where molecular hydrogen exists.

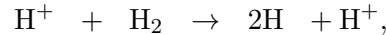
From the graphs in Janev et al. 1987, (2.2.5) it is evident that also



will be dominated by the above reaction 14. Please note that the rate coefficient of reaction 2.2.6 in Janev et al. 1987 is a factor 10 to high! (Personal communication with Bill Langer, 1995)

### 5.8.2. Dissociation of Molecular Hydrogen by $\text{H}^+$

The positive hydrogen ion is able to destroy molecular hydrogen through the charge exchange reaction (11). The direct collisional dissociation,



has often been left out by former studies. We also were not able to find a rate coefficient for this reaction. However, one does not believe this to be important since

1. at low temperatures where a significant  $\text{H}_2$  fraction exists there will be nearly no free protons due to the high recombination rate at low temperatures.
2. dissociation by electrons is likely to be more effective due to their higher velocities in the single temperature fluid.

### 5.8.3. Dissociation of Molecular Hydrogen by He

Dove and Mandy (1986b) found that He in comparison to  $\text{H}$  is very inefficient in dissociating  $\text{H}_2(0,0)$ . They further state that, evidently the collision between two closed shell species tends to cause the molecular bond to stiffen, whereas a collision with an atom weakens and loosens the molecular bond. In a follow up paper Dove et al. (1987) applied their result to interstellar densities and found that the dissociation through neutral helium is negligible and that  $\text{H}_2$ -He collisions do not excite the vib./rot. populations of  $\text{H}_2$  in low density gas. Following these results we do not include dissociation of  $\text{H}_2(0,0)$  by He.

#### 5.8.4. Dissociation of Molecular Hydrogen by $He^+$

The number fraction of  $He^+$  in primordial gas is about 10%. Due to the high ionization threshold of  $He^+$  of 54.4eV it will not be abundant at low temperatures. Furthermore, from the scaling relations of the rate coefficients given in Janev *et al.* (1987), we know the dissociation of  $H_2$  by  $He^+$  occurs 0.35 times less than the corresponding proton reaction. Therefore we can safely conclude that this reaction can be omitted.

#### 5.8.5. Dissociation of Molecular Hydrogen by $H_2$

The dissociation rate coefficient for  $H_2$  is of the same order and temperature dependence as the one for dissociation by neutral hydrogen (Lepp and Shull, 1983). However we do not include this reaction since the  $H_2$  to H fraction (and hence the rate) is always smaller than  $\sim 10^{-2}$  and therefore negligible.

The study of Dove *et al.* (1987a,b) showed that, in the low-density limit, dissociation of molecular hydrogen by collisions with helium at temperatures in the range 2000 –  $10^4$  K is negligible compared to the  $H_2$  - H collisions. Only for temperatures close to  $10^4$  K do the two rates become of the same order. We can, however, still neglect this process since helium has a much smaller number density than hydrogen, and second we also expect dissociation via the charge exchange reaction with  $H^+$  to dominate at such high temperatures.

We do not know the rate for direct collisional dissociation of molecular hydrogen by protons. However, by simply looking at the rate coefficients for ionization of  $H_2$  and dissociation of  $H_2^+$  by protons (Janev *et al.* 1987, 3.2.5, 3.2.6) one sees that those rate coefficients drop drastically for temperatures below 10eV. Therefore, we are confident that dissociation by protons is negligible. For dissociation by  $He^{++}$  ions exactly the same arguments used for protons are valid (see Janev *et al.* 1987, 5.2.1, 5.2.3). In addition the charge exchange reaction between  $H_2$  and  $He^{++}$  is highly inefficient for temperatures below 100eV.

### 5.9. Collisional induced Absorption

Molecular hydrogen does not have an electric dipole moment in its ground electronic state. As a result absorption of photons can only take place via electric quadrupole transitions and low-density molecular hydrogen gas is essentially transparent throughout the visible and infrared part of the spectrum. However, each time a collision between two particles occurs, the interacting pair ( $H_2$  -  $H_2$ ,  $H_2$  - He,  $H_2$  - H) acts as a “virtual supermolecule” which due to its nonzero electric dipole, can absorb photons with a probability which is much higher than that of an isolated  $H_2$  molecule. However, this process can, according to the results of Lenzuni, Chernoff, and Salpeter (1991), only contribute significantly to the opacity for number densities greater than  $\sim 10^{18} \text{ cm}^{-3}$ , and hence is negligible at the low densities considered here.

## 6. The Cooling and Heating Functions for Optical Thin Gas

To model the cooling behaviour of the gas correctly, we incorporate the following cooling and heating mechanisms,

- Compton cooling
- Recombination cooling due to hydrogen and helium
- Line cooling of hydrogen and helium



- Bremsstrahlung cooling
- Molecular formation and line cooling
- Photoionization heating
- Photodissociation heating

The cooling functions for Compton, recombination, line, and bremsstrahlung cooling we have used are given in AZAN96. The molecular cooling and heating rates are somewhat controversial in the literature and, therefore, deserve special attention.

## 6.1. Molecular Cooling

### Formation cooling of molecular Hydrogen

Most of the reaction enthalpy (1.83 eV for process 10 and 3.53 eV for process 8) goes rather into ro-vibrational excitation of the molecule than to the kinetic energy of the outgoing particles. We assume that all the reaction energy goes into excitation and gets radiated away through subsequent spontaneous decay to the ground state (Shapiro and Kang 1987), with the following cooling formula:

$$\Lambda_{H_2 \text{ Formation}} = n_H(3.53n_{H^-}k_8 + 1.38n_{H_2^+}) \text{ eV cm}^{-3} \text{ s}^{-1}$$

These reactions, however, are important heat sources at high densities ( $n \geq 10^8 \text{ 1/cm}^3$ ) where collisional de-excitation can transform most of the excitation energy into kinetic (thermal) energy. The density dependent heating rates are given by Hollenbach and McKee (1979, hereafter HM).

### Line Cooling of Molecular Hydrogen

Recently Martin, Schwarz, & Mandy (1996, MSM96 hereafter) have derived the molecular hydrogen cooling function for  $H_2 - H$  collisions with a complete set of rate coefficients. Their result differs substantially from former cooling functions (e.g. Hollenbach and McKee 1979; Lepp and Shull 1983). Especially at number densities exceeding  $10 \text{ cm}^{-3}$  Lepp and Shull's expression seems to overestimate (underestimate) the cooling at low (high) temperatures by an order of magnitude.

Although, the rate coefficients of MSM96 are only accurate for temperatures above 600 K, some of them have been found to agree with QCT calculations at 300 K. For lower temperatures, however, the MSM96 cooling function has to be understood as lower limit (personal communication with Peter Martin, 1996). **A FORTRAN77 routine that computes their fitting formula** (<http://zeus.ncsa.uiuc.edu:8080/abel/PGas/cool.html>) can be found on our WWW-Site. From Appendix B. we know that the number density of ortho- $H_2$   $n_2^o$  can be very small for applications where our model is valid. Therefore, if one were to estimate the cooling behavior to a high accuracy, a separate treatment of the ortho and para- $H_2$  states would be required.

### Photodissociation Heating

Our model includes the photodissociation processes of  $H_2$ , processes (27) and (28). Black and Dalgarno (1977) argue that, for typical radiation fluxes, the photodissociation by the two-step Solomon process (27) yields 0.4 eV per atom pair. Hence the corresponding heating function is

$$\Gamma_{27} = 6.4 \times 10^{-13} n_{H_2} k_{27} \text{ erg cm}^{-3} \text{ s}^{-1}. \quad (16)$$

For direct dissociation into the continua of the Lyman and Werner systems, the situation is similar to photoionization heating. Since the reaction channel leading to the excitation of the produced hydrogen atoms

is only accessible for excess photon energies greater than 10.2 eV, we can safely assume that all the excess energy of the dissociating photon will be shared as kinetic energies of the produced hydrogen atom pair. Hence the heating functions can be written,

$$\Gamma_{28} = n_{\text{H}_2} \int_{\nu_{th}}^{\infty} 4\pi\sigma_{28}(\nu) \frac{i(\nu)}{h\nu} (h\nu - h\nu_{th}) d\nu, \quad (17)$$

where  $i(\nu)$  denotes the radiation intensity and the integral is evaluated for the ortho and para-H<sub>2</sub> component separately because of their different threshold energies.

## 7. Application and Discussion of the Model

In this section we will use data from a 1d high resolution study of a cosmological sheet with wavelength 4Mpc, to discuss non-equilibrium effects and the chemical dynamics in primordial gas. The data is taken from Anninos & Norman 1996.

Very massive pancakes have strong virialization shocks ( $v_s \sim 100\text{km/s}$ ), which leads to the destruction of primordial pre-shock hydrogen molecules. The post shock gas cools faster than it recombines and leaves the gas with a significant free electron fraction even at low temperatures. This can clearly be seen in Figure 3 where the fractional abundances of all species in the post shock gas are plotted as a function of temperature. There we also see that H<sub>2</sub><sup>+</sup> is always much less abundant than H<sup>-</sup>. The doubly negative helium ion recombines very fast and therefore shows the non-equilibrium effect at somewhat lower temperatures than hydrogen. These abundances agree well with the ones given in Shapiro and Kang (1987).

### 7.1. H<sub>2</sub> Chemistry

The right hand side of an individual rate equation is, for collisional processes, given by a sum of terms  $k_{ij}n_in_j$ , where  $k_{ij}$  is the rate coefficient for the reaction between species  $i$  and  $j$ , which is taken positive if it produces the species under consideration, or negative if it destroys it. To see what processes dominate the chemistry of species  $l$ , let us consider the rate  $k_{ij}n_in_j$  divided by  $n_l$ , which we call rate per  $l$ -atom (molecule). Comparing this to the sum over all  $l$  producing/destroying processes (the evaluated right hand side) much insight about the ongoing processes can be gained. Actually this quantity equals the inverse reaction time scale and hence provides a measure of the time in which a particular species gets into equilibrium. We show such plots for H<sub>2</sub>, H<sub>2</sub><sup>+</sup>, and H<sup>-</sup> (Fig. 4, 6, and 5). The complete H<sub>2</sub> chemistry in our model is illustrated in Fig. 4. All molecular hydrogen producing reactions (8, 10, and 19) are shown as solid lines as well as their sum (labeled formation). The destroying processes (11, 12, and 13) are depicted by dashed – dotted lines. It is clear that the molecular hydrogen abundance at temperatures above  $\sim 7000$  K is a result of the balance between producing and destroying processes, what one could call a “collisional equilibrium”. It can also be seen that from 0.5eV to 1eV the charge exchange reaction of H<sub>2</sub> and free protons is the most efficient molecular hydrogen destruction path. At higher temperatures, molecular hydrogen are destroyed most efficiently by free electrons. Obviously here in the pancake collapse, destruction by neutral hydrogen atoms has a negligible influence on the molecular hydrogen abundance, which is certainly due to the high (non-equilibrium) abundance of free protons which will not be found as drastically enhanced, compared to the equilibrium abundances, for weak shock waves. For the production of H<sub>2</sub> we find that proc. 8 and 19, are always dominated by the fast H<sup>-</sup> formation path (proc. 8).

In summary, we find that the molecular hydrogen fraction is governed dominantly by three processes. Formation via H<sup>-</sup>, destruction through charge exchange with free protons, and destruction by free electrons. These insights can be used also for analytical estimates of the molecular hydrogen fraction during pancake collapse.

Let us illustrate this briefly on the molecular hydrogen abundance for temperatures,  $7000 \text{ K} \leq T \leq 10^4 \text{ K}$ . Here the  $\text{H}_2$  abundance can obviously be derived through the equilibrium condition  $dn_{\text{H}_2}/dt = 0$  with,

$$\frac{dn_{\text{H}_2}}{dt} \simeq k_8 n_{\text{H}^-} n_{\text{H}} - k_{11} n_{\text{H}_2} n_{\text{H}^+} = 0, \Rightarrow n_{\text{H}_2} \simeq \frac{k_8}{k_{11}} \frac{n_{\text{H}^-}}{x}$$

where  $x$  denotes the ionized fraction. Looking up the rate coefficients we can read off the qualitative temperature dependence and find that with a decreasing temperature in the range  $6000 \text{ K} \leq T \leq 2 \times 10^4 \text{ K}$ , the molecular hydrogen abundance increases. For lower temperatures, collisional processes are not efficient enough in destroying molecular hydrogen and it will get produced as long as there exists a significant amount of  $\text{H}^-$  ions at the level of a few percent.

## 7.2. The $\text{H}^-$ and $\text{H}_2^+$ Chemistry

The  $\text{H}^-$  ion is found to get into chemical equilibrium faster than the dynamical time scales (Courant, free-fall, and cosmological times). Hence the overall destruction and production lines in Fig. 5 are right on top of each other. Our model includes one  $\text{H}^-$  producing reaction, the radiative attachment (proc. 7), and six destroying reactions. Fig. 5 clearly illustrates that the processes 17 and 19 play no role, processes 15 and 16, little role, and processes 7, 8, and 14 the main role, for the  $\text{H}^-$  chemistry. Since the atomic data we used for the main processes 7, 8, and 14 are very accurate at all temperatures we ensured that the model will give also accurate predictions for the  $\text{H}^-$  abundance. An analogous plot for the  $\text{H}_2^+$  chemistry is given with Fig. 6. Obviously  $\text{H}_2^+$  has been in chemical equilibrium for all temperatures in our pancake study. All of its three production mechanisms contribute in individual temperature regimes. The radiative association reaction proc. 9 contributes strongly for temperatures below a few thousand Kelvin and dominates at higher temperatures as  $\sim 2 \times 10^4 \text{ K}$ . For the remaining interval charge exchange between  $\text{H}_2$  and  $\text{H}^+$  is the dominant  $\text{H}_2^+$  producing reaction. Furthermore it is clear from Fig. 6 that one can safely neglect the destroying mechanism proc. 19, because it does not contribute significantly, at any temperature, to the overall destruction of  $\text{H}_2^+$ . It is also evident that at all temperatures below  $\sim 8 \times 10^3 \text{ K}$  nearly every  $\text{H}_2^+$  molecule that gets produced will be converted to a neutral hydrogen molecule by proc. 10. At higher temperatures  $\text{H}_2^+$  will be destroyed by electrons. The data of Schneider *et al.* for the rate coefficient of this process, and consequently our fit, is quite inaccurate at such high temperatures and we do not expect the  $\text{H}_2^+$  abundance at temperatures higher than  $10^4 \text{ K}$  to be reliable. We see that process 19 was never important in determining the abundances of  $\text{H}^-$ ,  $\text{H}_2^+$ , and of  $\text{H}_2$ , and can therefore be neglected in future applications.

## 7.3. A Minimal Model

From the preceding section we clearly see that not all reactions are equally important. We devised a minimal model that incorporates only the essential processes need to accurately model the formation of molecular hydrogen. From Figure 4 it is evident that the only reaction involving  $\text{H}_2^+$  which contributes strongly to the  $\text{H}_2$  chemistry is the charge exchange reaction (11). Its rate is independent of the  $\text{H}_2^+$  abundance since it is a  $\text{H}_2^+$  producing reaction and we can conclude that at least for strong shocks the  $\text{H}_2$  abundance is independent of the  $\text{H}_2^+$  chemistry. For a minimal model we can use this and leave out reactions 9, 10, 17, and 19 so as to avoid solving a  $\text{H}_2^+$  rate equation. Further by looking at Figure 5 we find the process (15) to be negligible and process (16) only to be marginally important. Clearly (13) can be left out as well since it obviously does not contribute to the  $\text{H}_2$  chemistry. Furthermore, we note that it is not necessary to include the contributions from the reaction involving  $\text{H}^-$  and  $\text{H}_2$  to the major species H, He, and their ions. With these simplifications we eliminated 7 of the 19 reactions and reduced the reaction network to the following,

$$\frac{dn_{\text{H}}}{dt} = k_2 n_{\text{H}^+} n_e - k_1 n_{\text{H}} n_e \quad (18)$$

$$\frac{dn_{\text{H}^+}}{dt} = k_1 n_{\text{H}} n_e - k_2 n_{\text{H}^+} n_e \quad (19)$$

$$\frac{dn_{\text{He}}}{dt} = k_4 n_{\text{He}^+} n_e - k_3 n_{\text{He}} n_e \quad (20)$$

$$\frac{dn_{\text{He}^+}}{dt} = k_3 n_{\text{He}} n_e + k_6 n_{\text{He}^{++}} n_e - k_4 n_{\text{He}^+} n_e \quad (21)$$

$$\frac{dn_{\text{He}^{++}}}{dt} = k_5 n_{\text{He}^+} n_e - k_6 n_{\text{He}^{++}} n_e \quad (22)$$

$$\frac{dn_{\text{H}_2}}{dt} = k_8 n_{\text{H}^-} n_{\text{H}} - n_{\text{H}_2} (k_{11} n_{\text{H}^+} + k_{12} n_e), \quad (23)$$

where the number density of  $\text{H}^-$  is given by the equilibrium condition

$$n_{\text{H}^-} = \frac{k_7 n_{\text{H}} n_e}{k_8 n_{\text{H}} + k_{16} n_{\text{H}^+} + k_{14} n_e}. \quad (24)$$

To derive the number density of  $\text{H}^-$  by its equilibrium value is justified by comparing the figures, 4 and 5. Since they show the inverse of the reaction time scales of the different processes it is clearly evident that all reactions determining the  $\text{H}^-$  abundance occur on much faster time scales than those responsible for the  $\text{H}_2$  chemistry. We have checked this minimal model extensively and find the  $\text{H}_2$  abundance to generally agree with the full model to within a few percent over the entire temperature of the individual application.

## 8. Conclusions

We have derived a reliable time dependent chemistry and cooling model for primordial gas that, in connection with our new numerical method (AZAN96), proves as a powerful tool to investigate primordial structure formation in multidimensional numerical calculations. The model is designed to be applicable for densities below  $10^4 \text{ cm}^{-3}$  and temperatures  $< 10^8 \text{ K}$ . We have discussed the influence of the orth- $\text{H}_2$  to para- $\text{H}_2$  ratio on the cooling behaviour of the gas, derived new fits to molecular data, and developed a minimal model capable of describing primordial gas in applications where no external radiation fields are considered.

## 9. Related Websites

At our WWW-Site, **The LCA Cooling Model** (<http://zeus.ncsa.uiuc.edu:8080/abel/PGas/LCA-CM.html>), we present all the used atomic and molecular data in great detail. Further we provide there FORTRAN routines that compute the rate coefficients and solve the rate equations. Tom Abel continues to collect molecular data related to primordial gas at **The Primordial Gas Chemistry Page** (<http://zeus.ncsa.uiuc.edu:8080/abel/PGas/>). Further **Dima Verners Atomic Data Page** (<http://www.pa.uky.edu/verner/atom.html>) represents a superb reference for atomic data.

We would like to thank Dimitri Mihalas, Mordecai-Mark MacLow, Zoltan Haiman, Max Tegmark, and Evelyne Roueff for helpful discussion. Furthermore, we are grateful for useful correspondence with Bill Langer, Phil Stancil, Jonathan Rawlings, Alex Dalgarno, Peter Martin, and Stephen Lepp. This work was done partly under the auspices of the Grand Challenge Cosmology Consortium funded by NSF grant ASC-9318185. Tom Abel happily acknowledges the hospitality of the Max Planck Institut für Astrophysik and the Instituto Astrofisica de Canarias where parts of this work have been completed.

## REFERENCES

- Aggarwal, K.M. 1983, MNRAS, 202, 15P-20P.
- Aldrovandi, S.M.V. & Pequignot, D. 1973, A&A, 25, 137.
- Allison, A.C. and Dalgarno, A. 1969, Atomic Data, 1, 91.
- Allison, A.C. and Dalgarno, A. 1970, *Atomic Data*, 1, 289-304.
- Anninos, P., Norman, M.L. 1994, ApJ, 429, 434.
- Anninos, P., Norman, M.L. 1996, ApJ, 460, 556.
- Anninos, P., Zhang, Y., Abel, T., and Norman, M.L. 1995, *submitted to NewA (AZAN96)*. ApJ304, 15-61.
- Bieniek, R.J. 1980, J. Phys. B, 13, 4405.
- Black, J.H. 1981, MNRAS, 197, 553-563.
- Browne, J.C. and Dalgarno, A. 1969, *J. Phys. B*, 2, 885.
- Capuzzo-Dolcetta, R., Di Fazio, A., and Palla, F. 1985, A&A, 145, 290-295.
- Cen, R. 1992, ApJS, 78, 341.
- Corrigan, S.J.B. 1965, J. Chem. Phys., 43, 4381.
- Couchman, H.M.P. 1985, MNRAS, 214, 137-139.
- Couchman, H.M.P. and Rees, M.J. 1986, MNRAS, 221, 53.
- Dalgarno, A. and Lepp, S. 1987, in *Astrochemistry*, eds. Vardya, M.S. and Tarafdar, S.P. (Dordrecht:Reidel), 109-120.
- De Jong, T. 1972, A&A, 20, 263.
- Dolder, K. & Peart, B. 1985, Rep. Prog. Phys. 48, 1283-1332.
- Donahue, M. & Shull, J.M. 1991, ApJ, 383, 511-523.
- Dove, J.E. and Mandy, M.E. 1986, ApJ, 311, L93-96.
- Dove, J.E., Mandy, M.E., Sathyamurthy, N. and Joseph, T. 1986, *Chemical Physics Letters* Vol. 127, 1.
- Dove, J.E., Rusk, A.C.M., Cribb, P.H., and Martin, P.G. 1987, ApJ, 318, 379-391.
- Dunn, G.H. 1968, Phys. Rev., 171, p1.
- Ferland, G.J., Peterson, B.M., Horne, K., Welsh, W.F., and Nahar, S.N. 1992, ApJ, 387, 95-108.
- Haiman, Z., Thoul, A.A., & Loeb, A. 1996, ApJ, 464, 523.
- Hirasawa, T. 1969, *Progress of Theoretical Physics*, Vol. 42, No. 3, 523.
- Hollenbach, D. and McKee, C.F. 1979, ApJS, 342, 555-592.
- Hollenbach, D. and McKee, C.F. 1989, ApJ, 342, 306.
- Hummer, D.C., Stebbings, R.F., Fite, W.L., and Branscomb, L.M., 1960, *Phys. Rev.*, 119, 668.
- Hutchins, J.B., 1976, ApJ, 205, 103-121.
- Janev, R.K., Langer, W.D., Evans, Jr. K. and Post, Jr. D.E. 1987, *Elementary Processes in Hydrogen-Helium Plasmas* (Springer-Verlag).
- Jura, M. 1974, ApJ, 191, 378.

- Kang, H. and Shapiro, P.R. 1992, ApJ, 386, 432.
- Karpas, Z., Anicich, V., & Huntress, W.T.Jr. 1979, J. Chem. Phys. 70, 2877.
- Kashlinsky, A. and Rees, M.J. 1983, MNRAS, 205, p955-971.
- Launay, J.M., Le Dourneuf, M., & Zeippen, C.J. 1991, A&A, 252, 842-852.
- Lenzuni, P., Chernoff, D.F. and Salpeter, E.E. 1991, ApJS, 76, 759.
- Lepp, S., and Shull, J.M. 1983, ApJ, 270, 578-582.
- Mac Low, M.-M. and Shull, J.M. 1986, ApJ, 302, 585.
- Mandy, M.E., & Martin, P.G. 1993, ApJS, 86, 199.
- Martin, P.G., Schwarz, D.H., & Mandy, M.E. 1996, ApJ, 461, 265.
- Mitchell, G.F. and Deveau, T.J. 1983, ApJ, 266, 646-661.
- Moseley, J., Olson, R.E., and Peterson, J.R. 1975, *Case Studies in Atomic Physics*, vol.5 (Amsterdam: North-Holland), 1.
- Nakashima, K., Takagi, H., and Nakamura, H. 1987, J. Chem. Phys., Vol. 86, 726-737.
- Osterbrock, D.E. 1974, *Astrophysics of Gaseous Nebulae*, Freeman and Co., San Francisco.
- Osterbrock, D.E. 1989, *Astrophysics of Gaseous Nebulae and Active Galactic Nuclei.*, University Science Books, Mill Valley/California.
- Padmanabhan, T. 1993, *Structure formation in the universe*, Cambridge University Press.
- Peart, B., Bennett, M.A., and Dolder, K. 1985, Phys. B, 18, L439.
- Peebles, P.J.E. and Dicke, R.H. 1968, ApJ, 154, 891.
- Poulaert, G., Brouillard, F., Claeys, W., McGowan, J.W., and Van Wassenhove, G. 1978, J. Phys. B: Atom. Molec. Phys., Vol. 11, L671-673.
- Prasad, S.S., & Huntress, W.T., Jr. 1980, ApJS, 43, 1.
- Puy, D., Alecian, G., Le Bourlot, J., Leorat, J., & Pineau des Forets, G. 1993, A&A, 267, 337-346.
- Ramaker, D.E., and Peek, J.M. 1976, Phys.Rev.A, 13, 58.
- Rawlings, J.M.C., Drew, J.E. and Barlow, M.J. 1993, MNRAS, 265, 968-982.
- Rees, M.J. 1986, MNRAS, 222, 27P-32P.
- Rosenzweig, P., Parravano, A., Ibáñez, M.H. and Izotov, Yu.I. 1994, ApJ, 432, 485.
- Saslaw, W.C. and Zipoy, D. 1967, Nature, 216, 976-978.
- Schneider, I.F., Dulieu, O., Giusti-Suzor, A., & Roueff, E., 1994, ApJ, 424, 983-987.
- Senekowitsch, J., Rosmus P., Domcke, W. & Werner, H.J. 1984, Chem. Phys. Lett., 111, 211.
- Shapiro, P.R. and Kang, H. 1987, ApJ, 318, 32.
- Shull, J.M. 1978, ApJ, 219, 877-885.
- Shull, J.M. and McKee, C.F. 1979, ApJ, 227, 131-149.
- Stahler, S.W. 1986, PASP, 98, 1081.
- Stancil, P.C. 1994, ApJ, 430, 360-370.
- Stancil, P.C., Lepp, S., Dalgarno, A. 1996, ApJ, 458, 401-406.
- Stecher, T.P., & Williams, D.A. 1967, ApJ, 149, L29.

- Sun, Y. & Dalgarno, A. 1994, ApJ, 427, 1053-1056.
- Szucs, S., Karemara, M., Terao, M. 1983, *Proc. 13th Int. Conf. on Physics of Electronic and Atomic Collisions*, Berlin, ed. Eichler et al., (Amsterdam: North-Holland) Abstracts, 482.
- Szucs, S., Karemara, M., Terao, M., Brouillard, F.J., 1984, Phys. B, 17, 1631.
- Tegmark, M., Silk, J., Rees, M. J., Blanchard, A., Abel, T., Palla, P. 1996, to appear in ApJ, 473.** (<http://www.mpa-garching.mpg.de/max/minmass.html>)
- Tielens, A.G.G.M. and Hollenbach, D. 1985, ApJ, 291, 722.
- Verner Dima, 1996** (<http://www.pa.uky.edu/verner/atom.html>)
- Vietri, M., & Pesce, E. 1995, ApJ, 442, 618-627.
- Wadehra, J.M. and Bardsley, J.N. 1978, Phys.Rev.Lett, 41, 1795-1798.
- Wishart, 1979, MNRAS, 187, 59P-60P.
- Zhang, Y. & Anninos, P., & Norman, M.L. 1995, ApJ, 453, 57Z.
- Zhang, Y., Anninos, P., Abel, T., & Norman, M.L. 1996, *submitted to NewA*.

## A. Reactions and Rates

Here we present all the rate coefficients used in our model. All fits are accurate for temperatures ranging from 1K to  $10^8$  K. Since we are interested in numerical applications we did pay more attention to the accuracy of the fits than to the simplicity of the formulas. **A FORTRAN program that computes these rate coefficients** (<http://zeus.ncsa.uiuc.edu:8080/abel/PGas/LCA-CM.html>) can be obtained at our WWW site. The temperatures are in eV unless stated otherwise.

Table 1: *Collisional Ionization and Radiative Recombination of Hydrogen and Helium.*

(1)	<u><math>H + e^- \rightarrow H^+ + 2e^-</math></u>	Janev et al. 1987 (2.1.5)
	$k_1 = \exp[-32.71396786 + 13.536556 \ln(T) - 5.73932875 \ln(T)^2 + 1.56315498 \ln(T)^3 - 0.2877056 \ln(T)^4 + 3.48255977 \times 10^{-2} \times \ln(T)^5 - 2.63197617 \times 10^{-3} \times \ln(T)^6 + 1.11954395 \times 10^{-4} \ln(T)^7 - 2.03914985 \times 10^{-6} \ln(T)^8] \text{ cm}^3 \text{ s}^{-1}.$	
(2)	<u><math>H^+ + e^- \rightarrow H + \gamma</math></u>	Our fit to data given by Ferland et al. (1992)
	$k_2 = \exp[-28.6130338 - 0.72411256 \ln(T) - 2.02604473 \times 10^{-2} \ln(T)^2 - 2.38086188 \times 10^{-3} \ln(T)^3 - 3.21260521 \times 10^{-4} \ln(T)^4 - 1.42150291 \times 10^{-5} \ln(T)^5 + 4.98910892 \times 10^{-6} \ln(T)^6 + 5.75561414 \times 10^{-7} \ln(T)^7 - 1.85676704 \times 10^{-8} \ln(T)^8 - 3.07113524 \times 10^{-9} \ln(T)^9] \text{ cm}^3 \text{ s}^{-1}.$	
(3)	<u><math>He + e^- \rightarrow He^+ + 2e^-</math></u>	Janev et al. 1987 (2.3.9)
	$k_3 = \exp[(-44.09864886 + 23.91596563 \ln(T) - 10.7532302 \ln(T)^2 + 3.05803875 \ln(T)^3 - 0.56851189 \ln(T)^4 + 6.79539123 \times 10^{-2} \ln(T)^5 - 5.00905610 \times 10^{-3} \ln(T)^6 + 2.06723616 \times 10^{-4} \ln(T)^7 - 3.64916141 \times 10^{-6} \ln(T)^8) \text{ cm}^3 \text{ s}^{-1}.$	
(4)	<u><math>He^+ + e^- \rightarrow He + \gamma</math></u>	Cen (1992) and Aldrovandi & Pequignot (1973)
	$\begin{aligned} \text{Radiative : } k_{4r} &= 3.925 \times 10^{-13} T^{-0.6353} \text{ cm}^3 \text{ s}^{-1} \\ \text{Dielectronic : } k_{4d} &= 1.544 \times 10^{-9} T^{-\frac{3}{2}} \exp\left(-\frac{48.596 \text{ eV}}{T}\right) \left[0.3 + \exp\left(\frac{8.10 \text{ eV}}{T}\right)\right] \text{ cm}^3 \text{ s}^{-1}. \end{aligned}$	
(5)	<u><math>He^+ + e^- \rightarrow He^{++} + 2e^-</math></u>	Aladdin Database (1989)
	$k_5 = \exp[-68.71040990 + 43.93347633 \ln(T) - 18.4806699 \ln(T)^2 + 4.70162649 \ln(T)^3 - 0.76924663 \ln(T)^4 + 8.113042 \times 10^{-2} \ln(T)^5 - 5.32402063 \times 10^{-3} \ln(T)^6 + 1.97570531 \times 10^{-4} \ln(T)^7 - 3.16558106 \times 10^{-6} \ln(T)^8] \text{ cm}^3 \text{ s}^{-1}.$	
(6)	<u><math>He^{++} + e^- \rightarrow He^+ + \gamma</math></u>	Cen (1992)
	$k_6 = 3.36 \times 10^{-10} T^{-\frac{1}{2}} \left(\frac{T}{1000 \text{ K}}\right)^{-0.2} \left(1 + \left(\frac{T}{10^6 \text{ K}}\right)^{0.7}\right)^{-1} \text{ cm}^3 \text{ s}^{-1}, \text{ where T is in K.}$	



Table 2: *The formation paths of H<sub>2</sub>.*

(7) H + e<sup>-</sup> → H<sup>-</sup> + γ This work from data by Wishart (1979)

$$k_7 = \begin{cases} 1.429 \times 10^{-18} T^{0.7620} T^{0.1523 \log_{10}(T)} T^{-3.274 \times 10^{-2} \log_{10}^2(T)} \text{ cm}^3 \text{ s}^{-1} & \text{for } T \leq 6000 \text{ K} \\ 3.802 \times 10^{-17} T^{0.1998 \log_{10}(T)} \text{dex} \left( 4.0415 \times 10^{-5} \log_{10}^6(T) - 5.447 \times 10^{-3} \log_{10}^4(T) \right) \text{ cm}^3 \text{ s}^{-1} & \text{otherwise.} \end{cases}$$

(8) H + H<sup>-</sup> → H<sub>2</sub> + e<sup>-</sup> Our Integration of data from Janev et al. (1987)

$$\begin{aligned} T > 0.1 \text{ eV} : k_8 &= \exp[-20.06913897 + 0.22898 \ln(T) + 3.5998377 \times 10^{-2} \ln(T)^2 - \\ & 4.55512 \times 10^{-3} \ln(T)^3 - 3.10511544 \times 10^{-4} \ln(T)^4 + 1.0732940 \times 10^{-4} \ln(T)^5 - \\ & 8.36671960 \times 10^{-6} \ln(T)^6 + 2.23830623 \times 10^{-7} \ln(T)^7] \text{ cm}^3 \text{ s}^{-1}. \\ T < 0.1 \text{ eV} : k_8 &= 1.428 \times 10^{-9} \text{ cm}^3 \text{ s}^{-1}. \end{aligned}$$

(9) H + H<sup>+</sup> → H<sub>2</sub><sup>+</sup> + γ Shapiro & Kang (1987)

$$k_9 = \begin{cases} 3.833 \times 10^{-16} \times T^{1.8} \text{ cm}^3 \text{ s}^{-1}, & \text{for } T < 0.577 \text{ eV}, \\ 5.81 \times 10^{-16} \times (0.20651 T)^{-0.2891 \times \log(0.20651 \times T)} \text{ cm}^3 \text{ s}^{-1}, & \text{for } T \geq 0.577 \text{ eV}. \end{cases}$$

(10) H<sub>2</sub><sup>+</sup> + H → H<sub>2</sub> + H<sup>+</sup> Karpas et al. (1979)

$$k_{10} = (6.4 \pm 1.2) \times 10^{-10} \text{ cm}^3 \text{ s}^{-1}.$$

Table 3: *Other Collisional Processes involving  $H^-$ ,  $H_2^+$ , and  $H_2$ .*

(11) $\underline{H_2 + H^+ \rightarrow H_2^+ + H}$	This work
$\ln(k_{11})$	$= -24.24914687 + 3.40082444 \ln(T) - 3.89800396 \ln(T)^2 + 2.04558782 \ln(T)^3 - 0.541618285 \ln(T)^4 + 8.41077503 \times 10^{-2} \ln(T)^5 - 7.87902615 \times 10^{-3} \ln(T)^6 + 4.13839842 \times 10^{-4} \ln(T)^7 - 9.36345888 \times 10^{-6} \ln(T)^8 \text{ cm}^3 \text{ s}^{-1}.$
(12) $\underline{H_2 + e^- \rightarrow 2H + e^-}$	Donahue and Shull (1991)
$k_{12}$	$= 5.6 \times 10^{-11} T^{\frac{1}{2}} \exp\left(-\frac{102,124 \text{ K}}{T}\right) \text{ cm}^3 \text{ s}^{-1},$ where T is in K.
(13) $\underline{H_2 + H \rightarrow 3H}$	Dove and Mandy (1986)
$k_{13}$	$= 1.067 \times 10^{-10} T^{2.012} \times \exp(-(4.463/T)(1 + 0.2472 T)^{3.512}) \text{ cm}^3 \text{ s}^{-1}.$
(14) $\underline{H^- + e^- \rightarrow H + 2e^-}$	Janev et al. (1987, 7.1.1)
$k_{14}$	$= \exp[-18.01849334 + 2.3608522 \ln(T) - 0.28274430 \ln(T)^2 + 1.62331664 \times 10^{-2} \ln(T)^3 - 3.36501203 \times 10^{-2} \ln(T)^4 + 1.17832978 \times 10^{-2} \ln(T)^5 - 1.65619470 \times 10^{-3} \ln(T)^6 + 1.06827520 \times 10^{-4} \ln(T)^7 - 2.63128581 \times 10^{-6} \ln(T)^8] \text{ cm}^3 \text{ s}^{-1}.$
(15) $\underline{H^- + H \rightarrow 2H + e^-}$	Our modification to the Janev et al. (1987) data
$T > 0.1 \text{ eV}$	$: k_{15} = \exp[-20.37260896 + 1.13944933 \ln(T) - 0.14210135 \ln(T)^2 + 8.4644554 \times 10^{-3} \ln(T)^3 - 1.4327641 \times 10^{-3} \ln(T)^4 + 2.0122503 \times 10^{-4} \ln(T)^5 + 8.6639632 \times 10^{-5} \ln(T)^6 - 2.5850097 \times 10^{-5} \ln(T)^7 + 2.4555012 \times 10^{-6} \ln(T)^8 - 8.0683825 \times 10^{-8} \ln(T)^9] \text{ cm}^3 \text{ s}^{-1},$
$T < 0.1 \text{ eV}$	$: k_{15} = 2.5634 \times 10^{-9} \times T^{1.78186} \text{ cm}^3 \text{ s}^{-1}.$
(16) $\underline{H^- + H^+ \rightarrow 2H}$	Dalgarno and Lepp (1987)
$k_{16}$	$= 7 \times 10^{-8} \left(\frac{T}{100\text{K}}\right)^{-\frac{1}{2}} \text{ cm}^3 \text{ s}^{-1},$ where T is in K.
(17) $\underline{H^- + H^+ \rightarrow H_2^+ + e^-}$	Our modification to fit of Shapiro and Kang (1987)
$k_{17}$	$= \begin{cases} 2.291 \times 10^{-10} T^{-0.4} \text{ cm}^3 \text{ s}^{-1}, & \text{for } T < 1.719 \text{ eV} \\ 8.4258 \times 10^{-10} T^{-1.4} \exp(-1.301/T) \text{ cm}^3 \text{ s}^{-1}, & \text{otherwise.} \end{cases}$
(18) $\underline{H_2^+ + e^- \rightarrow 2H}$	Our fit to the Schneider et al. (1994) data
$k_{18}$	$= \begin{cases} 1.0 \times 10^{-8} \text{ cm}^3 \text{ s}^{-1}, & \text{for } T < 617 \text{ K}, \\ 1.32 \times 10^{-6} T^{-0.76} \text{ cm}^3 \text{ s}^{-1}, & \text{for } T > 617 \text{ K}, \end{cases}$ where T is in K.
(19) $\underline{H_2^+ + H^- \rightarrow H_2 + H}$	Dalgarno and Lepp (1987)
$k_{19}$	$= 5 \times 10^{-7} \left(\frac{100 \text{ K}}{T}\right)^{\frac{1}{2}} \text{ cm}^3 \text{ s}^{-1},$ where T is in K.

Table 4: *Photoionization and Photodissociation.*

- (20)  $\underline{\text{H} + \gamma \rightarrow \text{H}^+ + \text{e}^-}$ ,  
(22)  $\underline{\text{He}^+ + \gamma \rightarrow \text{He}^{++} + \text{e}^-}$  Osterbrock (1974)

$$\sigma_{20,22} = \frac{A_0}{Z^2} \left( \frac{\nu}{\nu_{th}} \right)^4 \frac{\exp[4 - 4(\arctan \epsilon)/\epsilon]}{1 - \exp(-2\pi/\epsilon)}, \text{ where } A = 6.30 \times 10^{-18} \text{ cm}^2,$$

$$\epsilon = \sqrt{\nu/\nu_{th} - 1}, \quad h\nu_{th} = 13.6Z^2 \text{ eV}.$$

- (21)  $\underline{\text{He} + \gamma \rightarrow \text{He}^+ + \text{e}^-}$  Osterbrock 1974

$$\sigma_{21}^\nu = 7.42 \times 10^{-18} \left( 1.66 \left( \frac{\nu}{\nu_{th}} \right)^{-2.05} - 0.66 \left( \frac{\nu}{\nu_{th}} \right)^{-3.05} \right) \text{ cm}^2, \text{ for } \nu > \nu_{th}.$$

- (23)  $\underline{\text{H}^- + \gamma \rightarrow \text{H} + \text{e}^-}$  Shapiro and Kang (1987)

$$\sigma_{23} = 7.928 \times 10^5 (\nu - \nu_{th})^{\frac{3}{2}} \frac{1}{\nu^3} \text{ cm}^2, \text{ for } h\nu > h\nu_{th} = 0.755 \text{ eV}.$$

- (24)  $\underline{\text{H}_2 + \gamma \rightarrow \text{H}_2^+ + \text{e}^-}$  O'Neil and Reinhardt (1978)

$$\sigma_{24}^\nu = \begin{cases} 0, & \text{for } h\nu < 15.42 \text{ eV}, \\ 6.2 \times 10^{-18} h\nu - 9.4 \times 10^{-17} \text{ cm}^2, & \text{for } 15.42 \text{ eV} \leq h\nu < 16.50 \text{ eV}, \\ 1.4 \times 10^{-18} h\nu - 1.48 \times 10^{-17} \text{ cm}^2, & \text{for } 16.50 \text{ eV} \leq h\nu < 17.7 \text{ eV}, \\ 2.5 \times 10^{-14} (h\nu)^{-2.71} \text{ cm}^2, & \text{for } h\nu \geq 17.7 \text{ eV}. \end{cases}$$

- (25)  $\underline{\text{H}_2^+ + \gamma \rightarrow \text{H} + \text{H}^+}$  Our fit to Stancil (1994)

$$\log_{10}(\sigma_{25}^{GS}) = (-1.6547717 \times 10^6 + 1.8660333 \times 10^5 \ln(\nu) - 7.8986431 \times 10^3 \ln(\nu)^2 + 148.73693 \ln(\nu)^3 - 1.0513032 \ln(\nu)^4)$$

- (26)  $\underline{\text{H}_2^+ + \gamma \rightarrow 2\text{H}^+ + \text{e}^-}$  Shapiro and Kang (1987)

$$\log_{10}(\sigma_{26}) = -16.926 - 4.528 \times 10^{-2} h\nu + 2.238 \times 10^{-4} (h\nu)^2 + 4.245 \times 10^{-7} (h\nu)^3,$$

for 30 eV < hν < 90 eV.

- (27)  $\underline{\text{H}_2 + \gamma \rightarrow \text{H}_2^* \rightarrow \text{H} + \text{H}}$  This work

Neglecting selfshielding,  $k_{27} = 1.1 \times 10^8 j(\bar{\nu}) \text{ s}^{-1}$ ,  
where  $j(\bar{\nu})$ , is the radiationflux in  $\text{ergs s}^{-1} \text{ cm}^{-2}$  at  $h\bar{\nu} = 12.87 \text{ eV}$ .

- (28)  $\underline{\text{H}_2 + \gamma \rightarrow \text{H} + \text{H}}$  This work

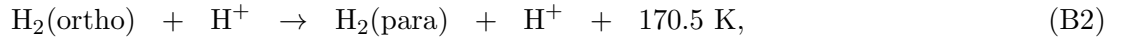
$$\sigma_{28} = \frac{1}{y+1} (\sigma_{28}^{L0} + \sigma_{28}^{W0}) + \left(1 - \frac{1}{y+1}\right) (\sigma_{28}^{L1} + \sigma_{28}^{W1})$$

## B. Ortho-H<sub>2</sub> to para-H<sub>2</sub> Ratio

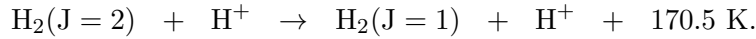
Many of the collisional rates have only been computed for the para configuration and are applicable only if para-H<sub>2</sub> is the dominant modification (Flower and Watt 1984, hereafter FW). For our purposes it plays another significant role in that its selection criteria for allowed rotational transitions are different. This is crucial to determine the exact cooling behavior at low temperatures, since low density primordial gas will cool mostly in the rotational lines  $E_3 - E_1 = 844.5\text{K}$  for the ortho configuration and  $E_2 - E_0 = 509.9\text{K}$  for para-H<sub>2</sub>. At formation the two different modifications will be abundant corresponding to their statistical weights, namely

$$\frac{n(\text{ortho})}{n(\text{para})} = \frac{n(J=1)}{n(J=0)} = 3. \quad (\text{B1})$$

FW argue for a single interconversion mechanism at low densities,



and suggest a temperature independent rate coefficient of,  $k_{op} = 3 \times 10^{-10} \text{ cm}^3 \text{ s}^{-1}$ . If the  $J=2$  state would be significantly populated, para-H<sub>2</sub> could be transformed to ortho by,



However, at the low density limit mostly the ground level will be populated and equ. (B2) will determine the ortho to para-H<sub>2</sub> ratio.

Assuming that we have a constant total number density of molecular hydrogen,  $n_2$ , the rate equation for para-H<sub>2</sub>,  $n_2^p$  simply becomes,

$$\frac{dn_2^p}{dt} = n_2^o n x k_{op}, \quad (\text{B3})$$

where  $n_2^o$ ,  $n$ ,  $x$ , denote the ortho-H<sub>2</sub> number density, the neutral hydrogen number density, and the ionized fraction respectively. The time evolution of the ionized fraction is determined from

$$\frac{dx}{dt} = -k_2 n x^2 \quad (\text{B4})$$

to be

$$x(t) = \frac{x_0}{1 + x_0 k_2 n t}. \quad (\text{B5})$$

Using  $n_2 = n_2^o + n_2^p$ , and equ. (B5), we derive the simple solution for the number density of para-H<sub>2</sub>

$$n_2^p = n_2 \left( 1 - \frac{3}{4} x_0^{k_{op}/k_2} x^{-k_{op}/k_2} \right) = n_2 \left( 1 - \frac{3}{4} x_0^{k_{op}/k_2} \left( n_H k_2 t + \frac{1}{x_0} \right)^{k_{op}/k_2} \right). \quad (\text{B6})$$

From this we clearly can see that if

- $k_{op} \ll k_2$ , ortho-H<sub>2</sub> to para-H<sub>2</sub> will not change within one recombination time.
- $k_2 \ll k_{op}$ , ortho-H<sub>2</sub> to para-H<sub>2</sub> will change dramatically within one recombination time.

Since  $k_2$  is well fitted by  $1.8 \times 10^{-10} T^{-0.65} \text{cm}^3 \text{s}^{-1}$ , it convincingly shows that always the latter case applies. Obviously the recombination time scale also sets the formation time scale of  $\text{H}_2$  since the electrons act as katalysts (see also Abel 1995, and Tegmark *et al.* 1996). Hence when  $\text{H}_2$  gets formed by the gas phase reactions (7) through (10), it might immediately get converted to its para configuration. The subsequent cooling of the gas will therefore happen mostly in the  $E_2 - E_0$  line of para- $\text{H}_2$ . For completely neutral hydrogen gas, however, at the low density and temperature limit the ortho- $\text{H}_2$  to para- $\text{H}_2$  ratio will be given by  $9 \exp(-170.5 \text{ K}/T)$  (Mandy & Martin 1993). Sun & Dalgarno (1994) computed the rate coefficients for odd transitions of low lying rotational levels by collisions with atomic hydrogen, in the temperature range 30 K – 1000 K. For temperatures below 300 K these reactions have rate coefficients  $\ll 10^{-17} \text{ cm}^3 \text{ s}^{-1}$ , i.e. for such low temperatures in low density gas ( $n_H \sim 1 \text{ cm}^{-3}$  the corresponding reaction time scales are  $\gg 10 \text{ Gyrs}$ . Hence if the gas can cool faster than it recombines below 300 K the above result is unchanged. However, the ortho- $\text{H}_2$  to para- $\text{H}_2$  will be different in different environments. Once the complete set of rate coefficients for collisional excitation and dissociation of  $\text{H}_2$  molecules by H atoms, given by Martin & Mandy (1995), are extended to temperatures below 450 K, and extended to  $\text{H}_2 - \text{H}_2$  collisions as well as  $\text{H}_2 - \text{H}^+$  reactions, it will be possible to study the ortho- $\text{H}_2$  to para- $\text{H}_2$  ratio in primordial gas for the entire range in which our reaction network is applicable. In summary, we would like to stress the need for a fit to the  $\text{H}_2$  cooling function that depends not only on temperature and density, but also on the ortho- $\text{H}_2$  to para- $\text{H}_2$  ratio.

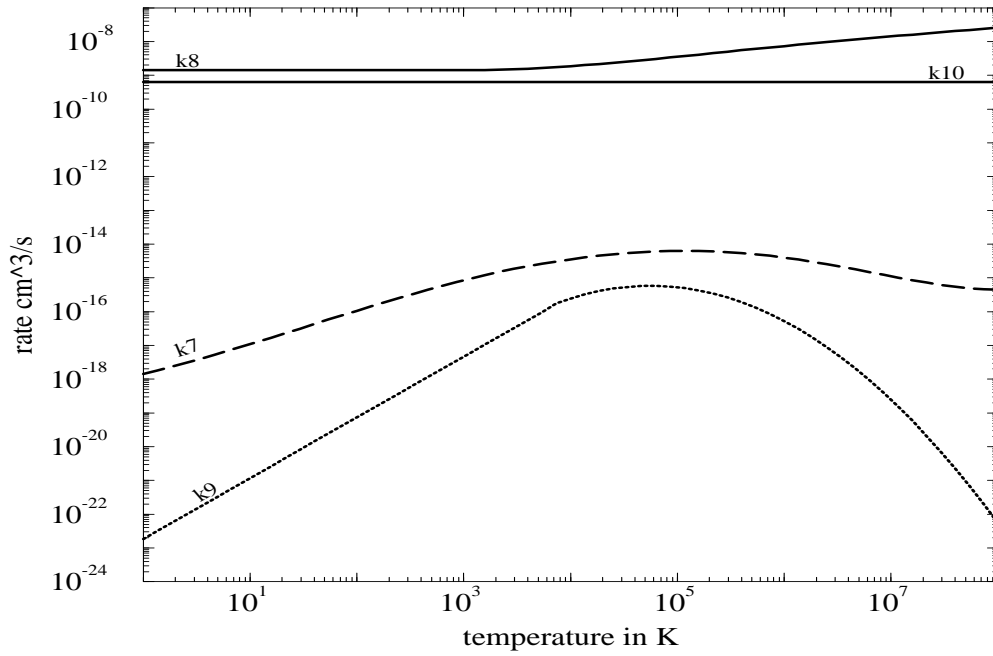


Fig. 1.— The rate coefficients for photo-attachment to  $\text{H}^-$  (dashed line),  $\text{H}_2^+$  formation (dotted line) and the two  $\text{H}_2$  forming reactions, proc. (8) and (10) (solid lines).

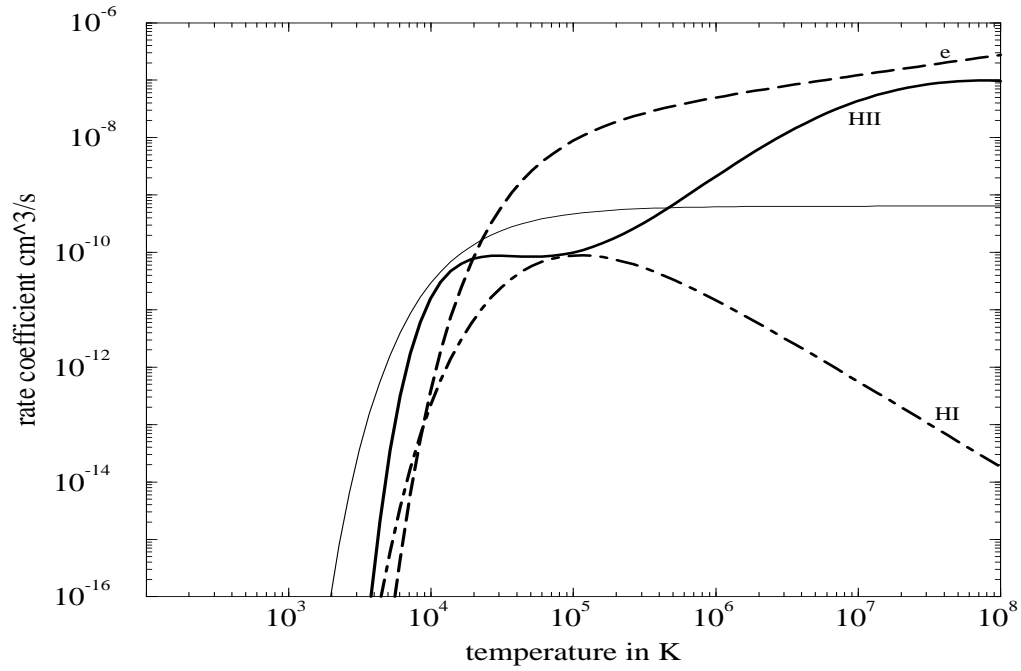


Fig. 2.— Rate coefficients for the dissociation of molecular hydrogen by neutral hydrogen (dot-dashed line), and free electrons (dashed line). The light solid line depicts the rate coefficient for charge exchange between  $H^+$  and  $H_2$ , given by Donahue and Shull (1991), whereas the thick solid line is our numerical integration from the Janev et al. data.

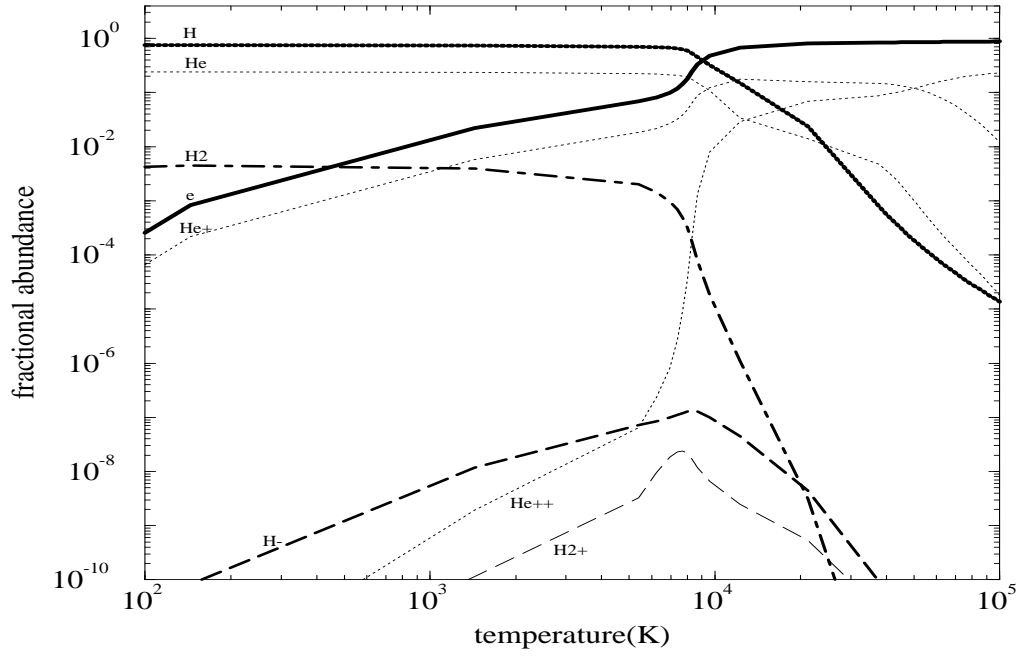


Fig. 3.— The fractional abundance of nine species in a collapsing pancake of wavelength 4 Mpc are shown vs. temperature. The data is taken from Anninos and Norman (1996). Clearly the non-equilibrium enhancement of free electrons at low temperatures can be seen. Note also the similar non-equilibrium behavior of the  $\text{He}^{++}$  fraction.



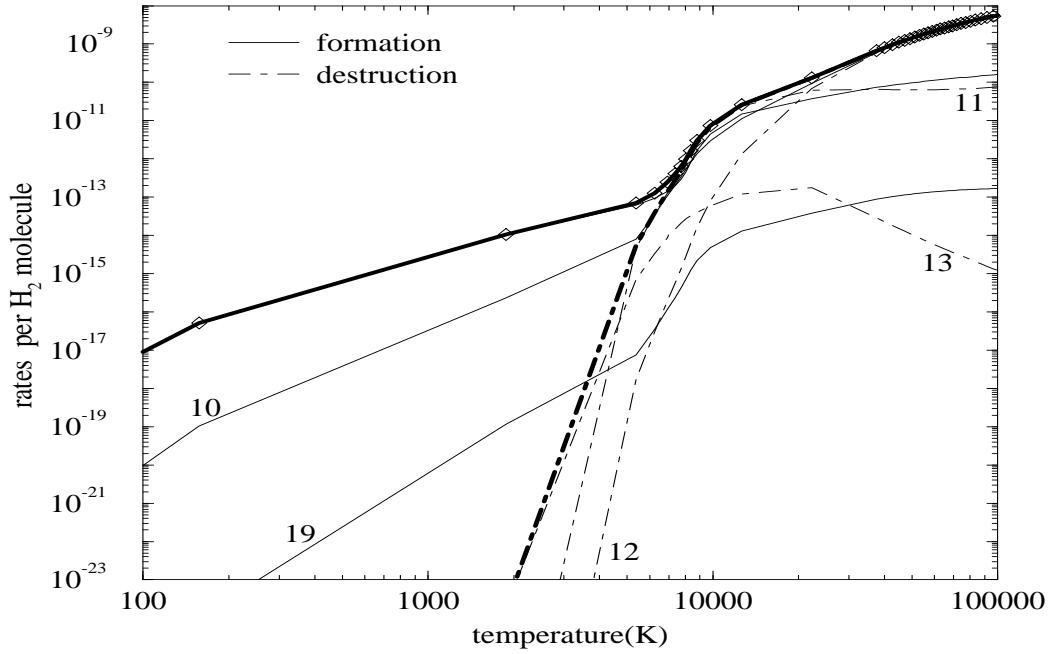


Fig. 4.— The inverse of the reaction time scale for all processes in our model, that involve hydrogen molecules. These relative rates for the producing collisional processes, (8), (10), and (19), are illustrated by solid lines. The H<sub>2</sub> destroying processes, (11), (12), and (13), are shown with dot-dashed lines. The thick solid (thick dot-dashed) line depicts the inverse of the sum of reaction time scales of all H<sub>2</sub> producing (destroying) processes. The divergence of these producing and destroying curves at low temperatures indicates that the H<sub>2</sub> molecules are out of equilibrium.

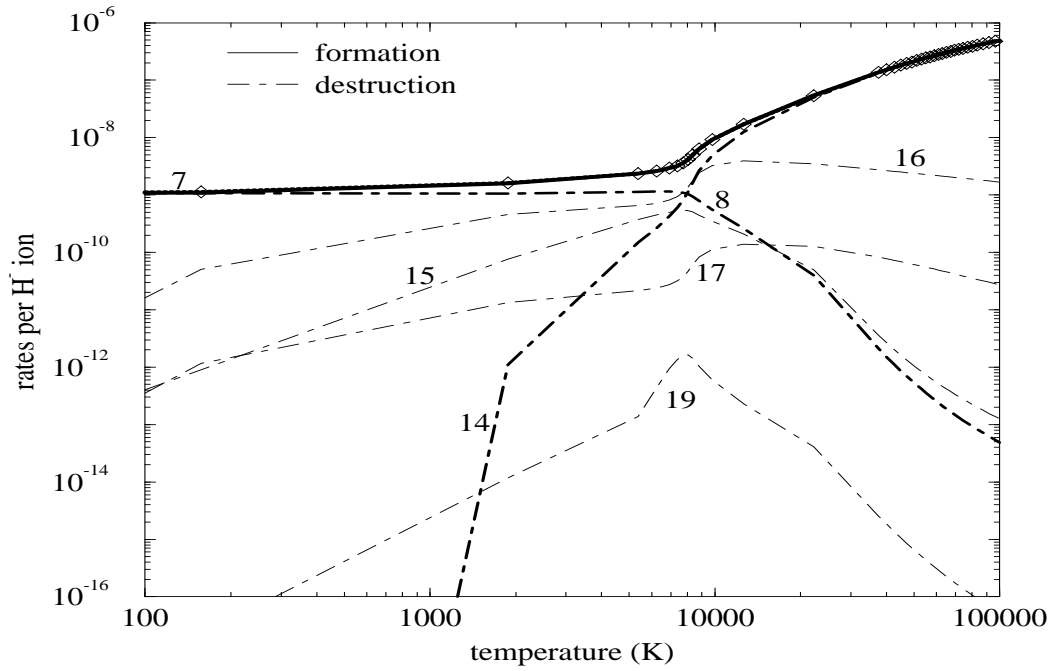


Fig. 5.— The relative rates are shown for the collisional processes involving  $\text{H}^-$ , including the single  $\text{H}^-$  producing reaction (7), and all its destruction processes (8), (14), (15), (16), (17), and (19). It is evident that  $\text{H}^-$  reached its equilibrium abundance within the hydrodynamical and cooling time scale since the sum of the production rates equals the sum of the destruction rates. Here the thick dot-dashed lines illustrate the major  $\text{H}^-$  destroying processes, (8) and (14).

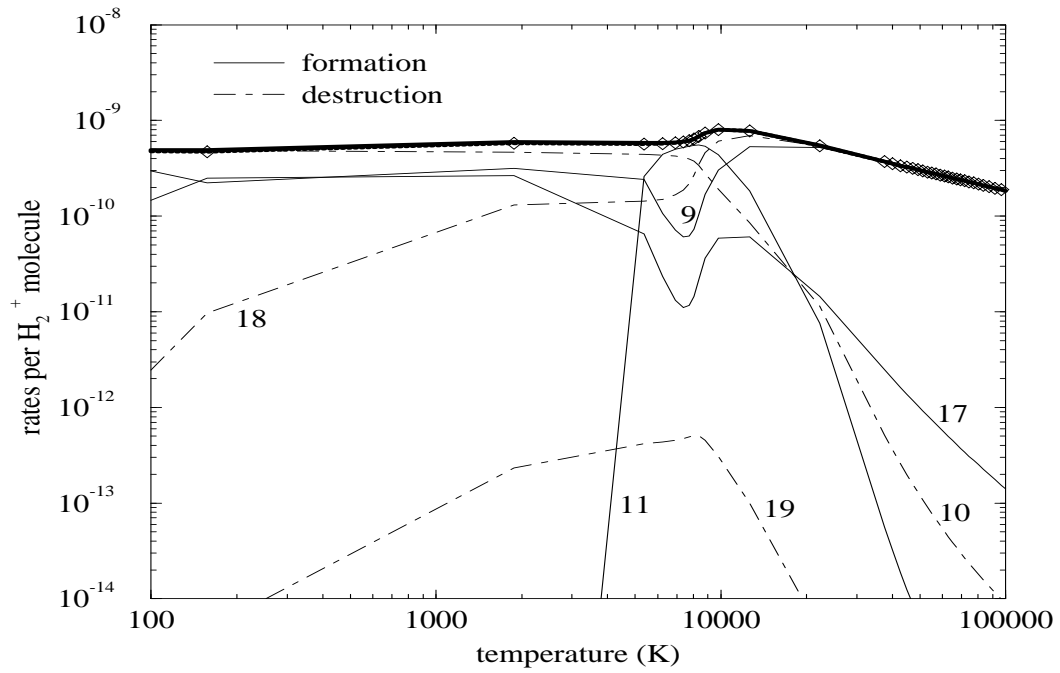


Fig. 6.— The inverse of the reaction time scale for the collisional processes involving  $\text{H}_2^+$ . The  $\text{H}_2^+$  producing processes (9), (11), and (17) are depicted by solid lines and the  $\text{H}_2^+$  destroying reactions (10, (18), and (19) correspond to the dot-dashed lines. Analogous to  $\text{H}^-$  (figure 5), it is clear that  $\text{H}_2^+$  reached its equilibrium abundance within the hydrodynamical and cooling time scales.